Universiteit Utrecht

Institute for Theoretical Physics

Master Thesis

Quantum Gravitational Fluctuations of Time Delay Observable in Minkowski Vacuum

Author:
Béatrice Bonga

Supervisors:
Prof. Dr. R. Loll
Dr. I. Khavkine

August 22, 2012

Abstract

In this thesis, I will discuss a clock synchronization thought experiment which models a diffeomorphism invariant time delay observable. For calculational purposes, the thought experiment takes place in an approximately Minkowski spacetime. The time delay observable is expanded to linear order in the gravitational field and its mean and variance are computed in the Fock vacuum of linearized quantum gravity. For the later calculation, we resorted to the use of computer algebra software due to the large amount of integrals that need to be evaluated. Divergences are regularized using a smearing procedure, which relies on the detector sensitivity profile. The results show that the quantum mean is given by $se^{-\theta}$ where s and θ are experimental input: s is the determining length scale and θ the hyperbolic rapidity between the worldlines of the lab and the probe. The leading order term of the quantum variance is proportional to $(s\ell_p/\mu)^2$ where μ determines the detector resolution. All circumstances alike, the quantum variance increases for increasing detector sensitivity. Additionally, the quantum variance is heavily influence by θ. The variance appears to become unbounded for small relative velocities. In particular, it changes by eight orders of magnitude between typical laboratory velocities and highly relativistic speeds. The observable was constructed to probe the causal structure of quantum spacetimes as well as serve as a benchmark to compare different approaches to quantum gravity.

Contents

Chapter 1

Introduction

In modern physics, a fundamental theory of quantum gravity that unifies quantum physics with general relativity (GR) is still an unsolved problem. Both quantum theory and GR have been experimentally verified numerous times, however, currently there exists no experimental evidence that allows us to see quantum gravitational effects. This may lead one to wonder why in the first place we want to quantize gravity. There are several motivations. First of all, quantum physics and GR can both be interpreted as "effective" theories: the prediction of experimental outcomes is limited to a specific physical context. Classical physics serves very well for predictions on macroscopic scales, but quantum mechanics is needed for an accurate description of nature at microscopic scales, i.e., atomic scales and smaller. GR is (presumed) to be a theory of the very large. Unifying both theories could provide us with a description of spacetime on all scales. Second, a motivation stemming directly from GR also indicates that a more general theory is needed. In spacetime regions with extreme curvature such as near the singularity inside a black hole and at scales relevant to early universe cosmology, the description of nature provided by GR breaks down. This is due to the spacetime singularities that occur in the solutions of GR. Thus, essential to understanding black holes and the initial state of the universe as described by cosmology a more general theory for GR is needed. Hopefully, quantum gravity may resolve these issues. The third motivation to quantize gravity comes from a more fundamental level. Any force field is partially determined by its sources, and the sources of gravity are matter fields, which are quantum mechanical. Therefore, gravity should also have a quantum mechanical nature. One could circumvent this argument by taking the expectation value of the matter stress-energy tensor, however, this view does not hold under the simplest interpretation of the observed anisotropies in the cosmic ray microwave background. For an extended explanation, see a review article by Woodard [1]. Fourth, there is good hope that this new more fundamental theory may provide us with deeper insights into our universe and may lead to predictions of new phenomena that may (eventually) be observed.

Many approaches have been developed over the years to find this theory of quantum gravity. (Super)string theory is one of the popular approaches. Other popular approaches are loop quantum gravity and asymptotic safety. But the list is much larger; just to name a few: covariant perturbation theory, canonical quantization method, the path integral approach, supergravity, twistor approach, causal dynamical triangulations and shape dynamics. A general review article by Carlip of various of these approaches is a good start [2]. None of these approaches has obtained the final full theory yet, as each approach has its own issues. However, in general there are two main problems that make the search for a theory of quantum gravity difficult. One is the dual role of the metric field $g_{\mu\nu}$: on the one hand it describes the dynamical aspects of gravity and on the other hand it gives us the background spacetime structure on which all the matter fields live. This suggests that in order to quantize the dynamical degrees of freedom of gravity, one also needs a quantum mechanical description of spacetime. There is no analogue with other quantum field theories that have the same requirement, as all theories are described

on a fixed background structure. Second, many mathematical problems arise in the search for a description of quantum gravity. Examples are its non-renormalizability and the difficulty of relating the mathematical framework with a clear physical interpretation.

In this thesis, the focus is on calculating quantum gravitational effects on a physical observable in the conservative setting of linearized gravity. We have chosen an observable with a clear physical interpretation and a tractable calculation by modeling a clock synchronization thought experiment in approximately Minkowski spacetime. The quantum mean and the variance of the observable are calculated. These results may serve as a benchmark to compare the predictions of various fundamental approaches to quantum gravity, by comparing how they agree with the conservative limit of quantum linearized gravity. Additionally, the observable is chosen such that it can probe the causal structure of spacetime. It should be noted that the work presented here is a continuation of previous work by Khavkine and builds heavily upon it [3].

The set-up of this thesis is as follows. First, issues related to modeling observables in classical an quantum physics are discussed in ch. 2. Next, in ch. 3 and 4 the specifics of the thought experiment are described closely following parts of work by Khavkine [3]. Ch. 5 deals with the explicit calculations and ch. 6 presents the results. Finally, a conclusion and outlook on possible future research is given in ch. 7. In the appendices, detailed mathematical derivations and results are presented that are used in the text.

Chapter 2

Modelling observables

The aim of physics, to describe the physical world around us and to predict future measurements, requires the pivotal concept of physical observables which are mathematical models of experimental outcomes. In this chapter, the difficulty of defining observables within the framework of general relativity is discussed first. Next, the requirements for observables in classical and quantum physics are described. Finally, the approach taken in my thesis is briefly outlined.

2.1 Observables in general relativity

To model a physical observable, there are two possible paths one could take: define a class of observables as broad as possible and take one observable from this class, or one could construct an explicit example without having first defined all possible observables.

The first route, to theoretically define a class of observables as general as possible is a difficult undertaking for GR. This is due to the fact that all observables are required to be invariant under spacetime diffeomorphisms. One could straightforwardly construct observables of the form

$$\int_M V_g \, f(\phi, g),$$

where M is the entire spacetime, V_g is the metric volume and $f(\phi, g)$ is a smooth spacetime scalar depending on the metric g and all other dynamic fields, denoted by ϕ. However, this class of observables is not likely to describe the outcome of any experiment that we are to perform since no experiment is able to take the effects of the entire universe into account. Additionally, there are some technical issues related to the convergence of such integrals. Another direct approach to define a class of observables as broad as possible is to take all possible solutions to the Einstein equations and divide out all solutions that are related by gauge transformations

$$\Gamma = S \,/\, D,$$

where Γ is the physical phase space, S is the solution space to Einstein's equations and D are all spacetime diffeomorphisms. In this way, the issues of the previous method are resolved, nonetheless, the class of observables obtained have no obvious physical interpretation. This is a result of the abstract nature of the construction of these observables. Hence, it is difficult to take an observable from a larger class of observables and start to do computations with it.

Therefore, in this thesis, we take the second path to model a physical observable: we start with an experimental set-up, check whether the observable that we are interested in is indeed spacetime diffeomorphism invariant and model the experimental outcome. This approach is clearly not as general as possible, but it allows one to study gravitational effects on a case by case basis. [3]

2.2 Observables in classical theories

In classical physics[1], the definition of observables as mathematical models of experimental outcomes can be made more rigorously.

Definition 1 *Let Γ be the space of initial data, i.e. the phase space. By means of a reduction procedure obtain the solution space S (which describes all dynamically possible solutions). All smooth continuous functions on this solution space S form an algebra of observables $\mathcal{A}$ over $\mathbb{R}$. Define Σ to be all normalized, positive linear functionals on this commutative classical algebra $\mathcal{A}$. Physical states σ are elements of Σ that satisfy the following three conditions*

1. *linearity $\sigma : \mathcal{A} \longrightarrow R$,*
2. *positivity $\sigma(f^2) \geqslant 0$ for any observable $f \in \mathcal{A}$,*
3. *normalization $\sigma(1) = 1$.*

Physical quantities at a given time t are calculated by evaluating the observable at the corresponding point in phase space. More concretely, consider a one-dimensional n-particle system, where the particles are specified at any time by their instantaneous positions and momenta, q and p, respectively. Thus, the phase space Γ is a $2n$-dimensional (smooth) manifold and an observable is any real-valued function on this phase space Γ. For example, the energy of a system is an observable. It can be calculated by evaluating the Hamiltonian function H at a given time at a point $x_t = (q_t, p_t)$

$$E = \int \mathrm{d}q \int \mathrm{d}p\, H(q,p)\delta(q - q_t)\delta(p - p_t),$$

where here the states of the system are the Dirac delta functions.

Multiple functions can be defined on a manifold. Two important operations with multiple functions on a manifold are multiplication and the Poisson bracket. The latter will be shown to be relevant not only to describe the dynamical evolution of observables, but it will also play an essential role in defining a class of quantum observables. Multiplication is defined pointwise $fg(x) = f(x)g(x)$ for $f, g \in C^\infty(M)$, $x \in M$ and M a smooth manifold. This multiplication is commutative, i.e. $fg(x) = gf(x)$. The Poisson bracket can be written as $\{f, g\}(x) = \pi^{ij}\partial_i f(x)\partial_j g(x)$. In canonical coordinates $x = (q, p)$, π^{ij} is represented by

$$\pi^{ij} = \begin{pmatrix} 0 & -I_n \\ I_n & 0 \end{pmatrix},$$

where I_n is the $n \times n$-identity matrix, and the Poisson bracket reduces to the often encountered one in classical mechanics

$$\{f, g\}(q, p) = \sum_{i=1}^{n} \left(\frac{\partial f}{\partial q_i}\frac{\partial g}{\partial p_i} - \frac{\partial f}{\partial p_i}\frac{\partial g}{\partial q_i} \right) \Bigg|_{q,p}.$$

There are three important properties that this Poisson bracket satisfies:

1. antisymmetry $\{f, g\} = -\{g, f\}$,
2. Leibniz rule $\{f, gh\} = \{f, g\}h + g\{f, h\}$,
3. Jacobi identity $\{f, \{g, h\}\} + \{g, \{h, f\}\} + \{h, \{f, g\}\} = 0$.

[1] Theories with gauge degrees of freedom are not considered here.

Evolution of a system is governed by the Hamilton equations, which for a general observable $f \in \mathcal{A}$ are

$$\dot{f} = \{f, H\},$$

where the dot on top of f indicates a time derivative and H is the Hamiltonian.

This can all be described in the context of symplectic manifolds or more generally using Poisson manifolds (M, α), where α is the Poisson tensor. (Symplectic manifolds are a subgroup of Poisson manifolds for which the Poisson tensor is non-degenerate, i.e. invertible.)

2.3 Observables in quantum theories

To make the step to quantum observables, which we are interested in, there are three possible roads to take. A common approach is the operator formalism in which quantum observables are operators in Hilbert space, physical states are linear combinations of the eigenfunctions of these operators and physical quantities are eigenvalues of these operators. Another method is the path-integral approach, which is generally used in quantum field theory. We shall follow the third road: deformation quantization, because it concentrates on "the central concepts of quantum theory: the algebra of observables and their dynamical evolution" [4, sec. I].

The requirements on the physical states and observables now slightly change.

Definition 2 *Let $\hat{\mathcal{A}}$ be a non-commutative quantum algebra of observables over $\mathbb{C}$, which can be obtained from all smooth functions on the reduced phase space endowed with a Poisson bracket. Define $\hat{\Sigma}$ to be all normalized, positive linear functionals on this non-commutative quantum algebra $\hat{\mathcal{A}}$. Physical states σ are elements of $\hat{\Sigma}$ satisfying the following three conditions:*

1. *linearity $\sigma : \hat{\mathcal{A}} \longrightarrow C$,*
2. *positivity $\sigma(f^* f) \geqslant 0$ for any observable $f \in \hat{\mathcal{A}}$,*
3. *normalization $\sigma(1) = 1$.*

In short, to go from the classical picture to the quantum picture we go from a commutative classical Poisson algebra of observables to a non-commutative quantum Poisson algebra. In the limit $\hbar \to 0$, the classical theory is obtained again.

Two central features of quantum theory are immediately obvious in this approach. First, the noncommutativity is present from the start and thus ensures that one cannot measure, for example, both the position and momentum of a particle at the same time to infinite accuracy. Second, the Heisenberg uncertainty is realized by describing physical states as distributions on phase space that are not sharply localized, in contrast to the classical case for which we had Dirac delta functions. To evaluate an observable, not just one point in phase space contributes, but in fact values of the observable in a whole region of phase space contribute and thus the resulting observable is an average value of the observable in a given state. [4]

To probe quantum gravitational effects, we need to construct a physical observable that satisfies all conditions placed on physical states from def. 2. Additionally, it should be invariant under spacetime diffeomorphisms. This is discussed in the next chapters.

Chapter 3

Thought experiment set-up

The aim of this project is to model an observable that can probe quantum gravitational effects. Obviously, we would like to have an experiment for which the effects due to quantum gravity are large. However, we do not know a priori which experiments will be most sensitive to quantum gravitational effects as we have no reliable calculation methods for a full theory of quantum gravity yet. Therefore, we chose a thought experiment that is simple and can be applied to any scale; from laboratory to cosmological scales. Furthermore, its physical interpretation is clear and its calculations are tractable. The experimental set-up of this simple thought experiment is described below and is obviously an idealization of a true experiment. The calculation of the observable in flat and in approximately flat Minkowski spacetime concludes this chapter.

3.1 Operational description

Consider two inertially moving, localized systems: the lab and the probe (see fig. 3.1). The lab and the probe are moving together, until at a certain moment the lab ejects the probe with a specified direction and relative velocity, where the moment, direction and relative velocity are all determined by the experimenter. Both the lab and the probe carry their own proper time clock, which at the moment of ejection O are synchronized to zero. After this moment, the lab and the probe continue to move inertially along their time-like geodesics and the probe starts sending time-stamped signals using an electromagnetic signal. This is done continuously in all directions. At a proper time interval s after ejection - determined by the experimenter, the lab records the time-stamped signal of the probe at time $\tau(s)$. The event of recording is called Q, and the corresponding event at which the recorded signal was emitted is called P.

The difference between the emission $\tau(s)$ and reception s time is the time delay observable that we seek

$$\delta\tau(s) = s - \tau(s).$$

In addition to its clean-cut physical interpretation, this observable has as an additional bonus: it allows one to probe the causal structure of spacetime. This is because this observable has to satisfy two important inequalities that are

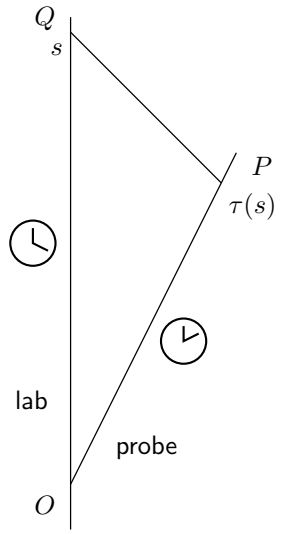

Figure 3.1: Geometry of the experimental protocol with the synchronization/ejection point O, the signal emission point P at time $\tau(s)$ after emission and the signal reception point Q at time s after emission.

closely related to the causal structure of spacetime. One of these inequalities is due to the maximality of the speed of light and requires that when the emission time is a smooth function of the reception time $\frac{d}{ds}\tau(s) > 0$. The second inequality requires $\delta\tau(s) \geq 0$ and is due to geodesic extremality. For proofs of these statements, see sec. IV in [3].

3.2 Mathematical description

In the preceding section, the experimental protocol was outlined. In this section, a mathematical description of the protocol is given which is taken from sec. III in [3].

Definition 3 *A* lab-equipped *spacetime (M, g, O, e_i^a) consists of an oriented, Lorentzian, time-oriented, globally hyperbolic, n-dimensional spacetime (M, g), a point $O \in M$ and an oriented orthonormal frame $e_i^a \in T_O M$, with a an abstract tensor index* [1] *and $i = 0, 1, \ldots, n$, where e_0^a is timelike and future directed.*

The lab worldline*, $Q(s) = \exp_O(su)$, is the geodesic passing through O with tangent vector $u^a = e_0^a$. Here $\exp_O \colon T_O M \to M$ is the usual geodesic exponential map.*

The probe worldline*, $P(t) = \exp_O(tv)$, is the geodesic passing through O with tangent vector $v^a = v^i e_i^a$, with $v^i \in \mathbb{R}^{1,3}$ a timelike, future directed, unit vector, chosen independent of the spacetime geometry.*

The signal worldline*, $Z(t, \lambda)$, is the null geodesic emanating from a point on the probe worldline, $Z(t, 0) = P(t)$, and intersecting the lab worldline, $Z(t, 1) = Q(s)$, with the earliest possible s (alternatively, if s is fixed, then t is chosen to be the latest possible).*

Physically, the point O represents the spacetime event when the probe is ejected from the lab. The vector e_0^a is tangent to the lab's worldline and e_i^a, $i = 1, 2, \ldots, n$ is the oriented spatial frame carried by the lab. Mathematically, all observables are modeled by a function on the space of lab-equipped spacetimes. In particular, the time delay observable is obtained from the functional relationship between the values of t and s when connected by Z:

Definition 4 *If t and s are such that $P(t)$ and $Q(s)$ are connected by $Z(t, \lambda)$, they are referred to as a pair of* emission *and* reception *times. The functional relationship between them is denoted*

$$t = \tau_v(s),$$

where $\tau_v(s)$ is called the recorded emission time *and the difference*

$$\delta\tau_v(s) = s - \tau_v(s),$$

is the time delay*.*

From this point on, we consider a four-dimensional lab-equipped spacetime and when the context is clear, the explicit dependence of the time delay observable on v and s is omitted. Furthermore, since s is determined by the experimenter we focus on calculating $\tau(s)$.

3.3 Calculation of time delay

Thus far, the time delay observable has been defined only implicitly. Since the time delay observable depends on the worldlines of the lab and the probe, an explicit expression for the time delay observable varies depending on the spacetime in which the experiment is realized. Calculations

[1] In the abstract tensor index, if we consider the vector v^a, the index a of this vector does not indicate a component of v in a particular basis as the usual coordinate tensor indices do. On the contrary, the index does not take any values in a set and is simply a label indicating that v is a vector (very similar to the arrow in $\vec{v}$). For more information on the distinction between abstract and coordinate tensor indices, see [5].

of worldines are difficult for arbitrary spacetimes, but for highly symmetric spacetimes geodesics can be exactly computed. To make calculations doable, we chose to perform the thought experiment in Minkowski spacetime with some perturbations on top of it. Other spacetimes such as the Schwarzschild metric or FRW-metric are not considered in this thesis, albeit worth investigation.

The following calculation has been carried out in two ways: using metric variables and vielbein variables. The results of both method agree. Since the vielbein formalism makes sense independently of the choice of coordinate chart and allows one to generalize the results more easily (though not directly relevant for this thesis), the calculation is presented using these variables. One such generalization is the inclusion of fermions on curved spacetimes, another is to an improved perturbation technique known as the Magnus expansion. The calculation in this section is heavily based on sec. V of [3].

3.3.1 Calculation in flat Minkowski spacetime

As a warm-up exercise, the calculation is first carried out in flat Minkowski spacetime. We consider $(M = \mathbb{R}^4, \eta, 0, \hat{x}_i^a)$ as our lab-equipped spacetime, where $\eta = \mathrm{diag}(-1, 1, 1, 1)$. Without loss of generality, we take arbitrary inertial coordinates x^i on (M, η) and use their origin as the moment of ejection and the vectors $\hat{x}_i^a = (\partial/\partial x^i)^a$ as our reference vierbein. The dual vierbein is $\hat{x}_a^i = (\mathrm{d}x^i)_a$ and is related to the reference vierbein by the identities $\hat{x}_i^a \hat{x}_a^j = \delta_i^j$ and $\hat{x}_i^a \hat{x}_b^i = \delta_a^b$. The Minkowski metric is defined via the pullback of η_{ij} by the dual vierbeins: $\eta_{ab} = \eta_{ij} \hat{x}_a^i \hat{x}_b^j$. Now the lab-equipped spacetime is completely specified, we need to construct our experimental set-up for which we need the worldlines of the lab and the probe in fig. 3.2. We parametrize these worldlines, respectively, as $x^i(s) = su^i$ and $x^i(t) = tv^i$ $(i = 0, 1, 2, 3)$, where u^i is the unit vector in the time direction, i.e. $u^i = (1, 0, 0, 0)$, and v^i is another time-like unit vector. The tangent vectors of these worldlines are related by the (positive) hyperbolic rapidity, which is defined in terms of the relative speed between the two worldlines, i.e. $v_{rel} = \tanh(\theta)$. Consequently, we have $u \cdot v = \eta_{ij} u^i v^j = -\cosh\theta$. The sides of the triangular set-up are

$$\begin{aligned} V^i &= tv^i, \\ U^i &= su^i, \\ W^i &= su^i - tv^i := w^i. \end{aligned}$$

Since W by construction is a light-like segment, we require $w^2 = 0$. This gives

$$\begin{aligned} w^i w_i = \eta_{ij} w^i w^j &= \eta_{ij}(su^i - tv^i)(su^j - tv^j) \\ &= -s^2 - 2st(u \cdot v) - t^2 \\ &= -s^2 + 2st\cosh\theta - t^2 \\ &= -s^2 + 2st(e^\theta + e^{-\theta}) - t^2 \\ &= -(se^\theta - t)(se^{-\theta} - t) = 0. \end{aligned}$$

Therefore, the retarded functional relation between the emission and reception time is given by

$$\tau_{cl}(s) = t = se^{-\theta},$$

where the subscript refers to classical, as it will serve as the classical background expectation for quantum fluctuations later on. This relation shows that the causal inequality $\frac{d}{ds}\tau(s) > 0$ is indeed satisfied. Also the second causal inequality, i.e. the time delay observable is always larger than or equal to zero, clearly holds since $e^{-\theta} < 1$ for all physically allowed θ.

3.3.2 Calculation in approximately Minkowski spacetime

We now consider Minkowski spacetime with perturbations on it. In accordance with the previous calculation, we first define our lab-equipped spacetime. Next, we describe our experimental set-up in this lab-equipped spacetime, after which we determine the functional relation between the

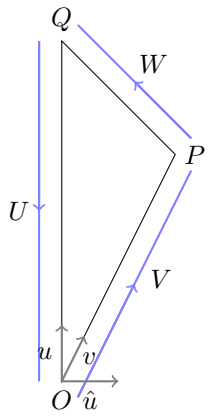

Figure 3.2: The set-up of the thought experiment: O denotes the origin (i.e., point of ejection), the oriented line segment OP is denoted by V, PQ by W and QO by U. The vectors $u, \hat{u}, v$ are all unit vectors defined at the origin.

emission and reception time. We keep the same underlying manifold M with reference vierbein $\hat{x}_i^a$ and same point of origin as in the flat case, but take another lab-equipped spacetime $(M, g, 0, \hat{e}_i^a)$. Any other vierbein on this manifold can be obtained by a general linear transformation

$$e_i^a = \bar{T}^{i'}{}_i \, \hat{x}_{i'}^a, \qquad e_a^i = T^i{}_{i'} \, \hat{x}_a^{i'}, \tag{3.1}$$

where T and $\bar{T}$ are spacetime dependent invertible matrices such that $\bar{T} = T^{-1}$. We take a transformed vierbein that satisfies

$$e_i^a e_a^j = \delta_i^j, \qquad e_i^a e_b^i = \delta_a^b,$$

and use this new orthonormal frame as the spacetime vierbein at the origin. Since our lab-equipped spacetime is approximately Minkowski spacetime, the transformation tensor T needs to be close to the identity matrix. This can be parametrized by $T = \exp(h)$ where we take h to be small (h can be thought of as the gravitational field). A logical choice for the lab-frame would be the spacetime vierbein at the origin, however, the lab-frame is not uniquely determined and can be obtained by yet another general linear transformation at the origin. That is,

$$\hat{e}_i^a = (T_O)_i^{i'} \hat{x}_{i'}^a,$$

where the hat indicates the lab-frame vierbein. The possible distinction between this lab-frame and the spacetime vierbein at the origin is

$$\hat{e}_i^a = L_i^{i'} e_{i'}^a \quad \text{with} \quad L_i^{i'} = (T_O)_j^{i'} T_i^j,$$

where L is a Lorentz transformation considering it satisfies $L_i^{i'} L_j^{j'} \eta_{i'j'} = \eta_{ij}$. Using the same reasoning as above for the transformation matrix, this Lorentz transformation can be parametrized as $\exp(h_O)$, where the subscript O indicates that the gravitational field needs to be evaluated at the origin. The metric clearly changes with regard to flat spacetime and is now defined via the pullback of η_{ij} by the spacetime vierbeins in eq. (3.1) (in contrast to the reference vierbeins in flat Minkowski space). The metric can be written to linear order in the gravitational field using the expression for the transformation tensor and expanding it

$$\begin{aligned} g_{ab} &= \eta_{ij} e_i^a e_j^b = \eta_{ij} T_{i'}^i T_{j'}^j \hat{x}_a^{i'} \hat{x}_b^{j'} \\ &= \eta_{ab} + (\eta_{i'j} h_{i'}^i + \eta_{ij'} h_{j'}^j) \hat{x}_a^{i'} \hat{x}_b^{j'} + \mathcal{O}(h^2) \\ &= \eta_{ab} + \tilde{h}_{ab}. \end{aligned}$$

Note the discrepancy between the deviation from Minkowski spacetime in vierbein (h_{ab}) and in metric (h_{ij}) variables

$$\tilde{h}_{ab} = 2h_{(ij)}\hat{x}^i_a\hat{x}^j_b + \mathcal{O}(h^2), \quad \text{where} \quad h_{ij} = \eta_{ij'}h^{j'}{}_j. \tag{3.2}$$

Now the lab-equipped spacetime is completely determined, we need to construct the experimental set-up. This is done by parallel propagating the tangent vector to the probe v along its timelike geodesic, after which a light-like vector, denoted w, which was also parallel propagated along this geodesic, is now parallel propagated along its own geodesic. Finally, the tangent vector to the lab u is parallel propagated along these two geodesics and then parallel propagated along its own time-like geodesic back to the origin. This experimental protocol requires that we know how to parallel propagate vectors along time-like and light-like worldlines. For parallel transportation of a vector $v^a(t)$ along a worldline $\gamma(t)$, in addition to knowledge of the geodesic, we need to know $v^a(0)$ at $\gamma(0)$. A geodesic is completely determined given the point of origin $\gamma(0)$ and initial tangent vector $\dot{\gamma}(0)$. Solutions for the geodesic and parallel propagation to linear order in the gravitational field are derived in app. B and will be used in the remaining part of this chapter.

In the flat case, the triangle was formed by the line segments (V, W, U) with tangent vectors $(tv^a, w^a, -su^a)$. In the present situation due to the presence of the gravitational field, the line segments are no longer straight lines but are slightly curved, which we will denote by putting tildes on all segments: $(\tilde{V}, \tilde{W}, \tilde{U})$ and, accordingly, $(\tilde{t}\tilde{v}^a, \tilde{w}^a, -\tilde{s}\tilde{u}^a)$. To be consistent with the experiment, we keep $\tilde{s} = s$, $\tilde{v} = v^i\hat{e}^a_i$ and $\tilde{u} = u^i\hat{e}^a_i$ fixed. Furthermore, $\tilde{w}^a$ should remain null and $\tilde{U}$ and $\tilde{V}$ need to intersect for the triangle needs to close. These first four requirements lead to the following equations

$$\tilde{s} = s, \tag{3.3}$$
$$\tilde{t} = e^{\tilde{r}}t, \tag{3.4}$$
$$\tilde{v}^a = v^i\hat{e}^a_i = e^a_i \exp(h_O)^i_j v^j, \tag{3.5}$$
$$\tilde{u}^a = e^a_i[\exp(p_U)\exp(p_W)\exp(p_V)]^i_j(h_O)^j_k u^k, \tag{3.6}$$
$$\tilde{w}^a = e^a_i \exp(\tilde{q})^i_j w^j, \tag{3.7}$$

where we have used $\exp(p_\gamma)$ to denote the parallel transport operator along γ as defined in eq. (A.7), and we parametrized the changes in $\tilde{t}$ and $\tilde{w}$ due to the curvature by $\exp(\tilde{r})$, where $\tilde{r}$ is a scalar and $\exp\tilde{q}$ is a Lorentz transformation, which both need to be determined yet. Since we are working at linear order, we only need the leading terms in the expansion of these unknowns

$$\tilde{q}^i_j = q^i_j + \mathcal{O}(h^2), \quad \tilde{r}^i_j = r + \mathcal{O}(h^2).$$

The only requirement left is the closure of the VWU triangle. Using the perturbative solution of the geodesic and parallel transport equations in terms of H and J obtained in app. B (eqs. (A.12) and (A.11))[2], at linear order, the triangle closure condition can be written out explicitly as

$$\begin{aligned} 0 = {} & tv^i + rtv^i + J^i_{V,\varnothing} \\ & + w^i + q^i_j w^j + J^i_{W,V} \\ & - su^i - H^i_j su^j + J^i_{U,VW} \end{aligned} \tag{3.8}$$
$$= rtv^i + q^i_j w^j - H^i_j su^i + J^i, \tag{3.9}$$

where we defined H and J in the above equation, analogue to the notation in eq. (A.14), as

$$\eta_{ik}H^k_j = H_{ij} = (H_{V,W,U})_{ij},$$
$$\eta_{ik}J^k = J_i = (J_{V,W,U})_i.$$

[2]For definitions of H and J, see app. B eq. (A.9) and eq. (A.13).

The first term on each line in eq. (3.8) vanishes due to the closure of the zeroth order geodesic triangle. Contracting the closure condition with w^i makes the term with q vanish (due to its antisymmetry). The solution for the first order correction to the emission time (which is given by r) is

$$r = -\frac{w^i J_i - w^i H_{ij} s u^j}{\tau_{\rm cl}(s) v \cdot w}, \tag{3.10}$$

where we substituted the zeroth order solution for t which is τ_{cl}.[3] This observable is indeed invariant under linearized diffeomorphisms. In particular, H and J are separately gauge invariant. This is checked in detail in the appendix of [3]. More explicitly, we have

$$\begin{aligned} w^i H_{ij} s u^i &= \sum_{X=V,W,U} \left(s w^i u^j \left[h_{[ij]} \right]_{x_1}^{x_2} + 2 s w^{[i} u^{j]} x^k \int_X \mathrm{d}t \, \partial_i h_{(kj)} \right), \\ w^i J_i &= \sum_{X=V,W,U} \left(-w^i x^j \int_X \mathrm{d}t \, h_{(ij)} + 2 w^{[i} x^{j]} x^k \int_X^{(1)} \mathrm{d}t \, \partial_i h_{(kj)} + \sum_{Y<X} 2 w^{[i} x^{j]} y^k \int_Y \mathrm{d}t \, \partial_i h_{(kj)} \right), \end{aligned}$$

where $\int^{(1)}$ indicates that the integral needs to be iterated, for details see app. B. The first term in the expression for H vanishes since we are working in a symmetric gauge. The more detailed expression for r is then given by

$$\begin{aligned} r = \frac{1}{\tau_{\rm cl}(s) v \cdot w} \Bigg(& 2 W^{[i} U^{j]} V^k \int_V \mathrm{d}t \, \partial_i h_{(kj)} + 2 W^{[i} U^{j]} W^k \int_W \mathrm{d}t \, \partial_i h_{(kj)} + 2 W^{[i} U^{j]} U^k \int_U \mathrm{d}t \, \partial_i h_{(kj)} \\ & + W^i V^j \int_V \mathrm{d}t \, h_{(ij)} - 2 W^{[i} V^{j]} V^k \int_V^{(1)} \mathrm{d}t \, \partial_i h_{(kj)} + W^i W^j \int_W \mathrm{d}t \, h_{(ij)} + W^i U^j \int_U \mathrm{d}t \, h_{(ij)} \\ & - 2 W^{[i} U^{j]} U^k \int_U^{(1)} \mathrm{d}t \, \partial_i h_{(kj)} - 2 W^{[i} U^{j]} W^k \int_W \mathrm{d}t \, \partial_i h_{(kj)} - 2 W^{[i} U^{j]} V^k \int_V \mathrm{d}t \, \partial_i h_{(kj)} \Bigg). \end{aligned} \tag{3.11}$$

Originally, in the part stemming from J there were two terms proportional to $W^{[i} W^{j]}$. These are not displayed as they unequivocally equal to zero.

For notational convience, from this point onwards we will use a more dense notation. Since by construction each term in r is linear in h, we write r as $r = r^x h_x$ where h_x represents the gravitational field and r^x is its tensorial coefficient that can contain vectors, tensors, integrals and derivatives. The x-index is shorthand for all tensorial indices. Being more specific, we can write the coefficient r^x as

$$r^x = \sum_{K,n,X} r^{Kij}_{|K| n X} \int_X^{(n)} \nabla_K, \tag{3.12}$$

where $|K|$ is a multi-index and denotes the number of derivatives (which is either zero or one), n the number of iterated integrals (which is zero, for a single integral, or one, for a single iterated integral) and X the line segment along which the integral needs to be evaluated (which is either V, W or U).

[3] The previously published expression for r in eq.(44) in [3] has a minus sign missing in front of the term proportional to H.

Chapter 4

Quantum effects

The description of the experimental set-up has thus far been completely classical. In this chapter, the step to quantum theory is made. Three issues related to this are briefly discussed first: the absence of a theory of quantum gravity, the issue of time observables in quantum physics and general concerns with regard to modeling measurements in quantum mechanics. Next, the smearing function is introduced to regularize the divergences that arise. Furthermore, an expression for the smeared first order corrections to the variance of the time delay observable is given. Finally, this work is compared to previous research.

4.1 Three issues related to quantum theory

At the moment, there is no full theory of quantum gravity. Since we do not want to assume any fundamental underlying theory for our results, we use the Fock quantization of the linearized gravitational field on a Minkowski background as our approximate theory of quantum gravity. This is reasonable following subsequent arguments. In the classical limit, quantum gravity should reproduce GR. This idea can be generalized for which we need two combine two ideas. One is that the dynamics of gravity under general circumstances (e.g., not too strong curvature) is very closely approximated by the dynamics of linearized gravity (as is the case for our experimental set-up). And second, there are many examples that show us that for any field theory whose dynamics is closely approximated by its linear theory, the Fock quantization of this linear theory is a very good approximation of the full quantum theory. An example of such a field theory, in elementary particle physics, is the Dirac field whose excitations describe free electrons. The canonical example in condensed matter physics is the (effective) phonon field. Other examples are spinons, magnons, exitons and plasmons. Merging these two ideas, we can deduce that in the appropriate limit and in regions of spacetime where the curvature is not too strong, quantum gravity should also reproduce quantum linearized gravity. Therefore, we use as our approximate theory of quantum gravity the Fock quantization of the linearized gravitational field.

Another issue that needs to be addressed is the issue of time in quantum physics. Pauli made an elegant argument why there exists no operator in quantum mechanics that corresponds to time [6]. The argument is as follows: imagine a quantum mechanical system with a Hamiltonian operator $\hat{H}$ whose spectrum is bounded from below. Let $\hat{T}$ be the operator corresponding to a time observable satisfying the commutation relation $\left[\hat{T}, \hat{H}\right] = i\hbar$ together with the appropriate continuity and functional analytic conditions. Then according to the Stone-von Neuman uniqueness theorem both $\hat{T}$ and $\hat{H}$ need to have an unbounded spectrum. This is in contradiction with the assumption that $\hat{H}$ has a bounded spectrum. Therefore, Pauli stated that no observable $\hat{T}$ exists that is related to a time observable. However, this line of reasoning is built on several assumptions that do not need to hold for all physical applications. One physical situation which circumvents this argument is when we have a Hamiltonian $\hat{H}$ that is not bounded from

below (e.g., a linear potential or a harmonic oscillator with an inverted potential—which would correspond, for instance, to a pen balancing on its top). Another physical application would be when we relax the commutation relation $[\hat{T}, \hat{H}] = i\hbar$ to $[\hat{T}, \hat{H}] \sim i\hbar$ where the equality may be restored by higher order corrections in $\hbar$ or may be small in other ways when restricted to physically relevant situations. An example of the latter situation is a particle on a circle. For this thought experiment, we imagine all clocks to have an unbounded spectrum and, consequently, Pauli's argument will not apply. This will clearly lead to stability issues in certain regimes, however, these are ignored. One could also take a more realistic system by picking a clock valued on a circle like an actual analog clock, which would put us in the second situation, where the commutation relation is relaxed [7, 3].

The third issue concerns modeling measurements in quantum mechanics. This requires a very precise outline of the experimental protocol since many measurements in quantum theory do not commute. For example, measuring observable A first and next observable B, may yield a different outcome than measuring observable A and B in the reversed order. Fortunately, there is a general consensus that these ordering ambiguities are of order $\hbar^2$ and higher orders in $\hbar$. Thus, they are not relevant for this calculation. For a more detailed discussion, see sec. VI, C of [3].

4.2 Smearing function

Having addressed these issues, being interested in calculating the emission time (and more generally, any function thereof), we would like to evaluate

$$\langle\psi|\hat{\tau}^n(s)|\psi\rangle, \quad \text{where} \quad n \in \mathbb{Z}$$

because any function can be approximated by a power series. For the state $|\psi\rangle$, we take the Poincaré invariant Fock vacuum $|0\rangle$, since it is a natural choice in Minkowski spacetime and simplifies the calculations significantly due to its symmetries. The Fock vacuum is a Gaussian state with respect to each mode of a harmonic oscillator. Considering that any linear field theory is merely a collection of coupled harmonic oscillators, the Fock vacuum is also Gaussian with respect to any observable linear in the gravitational field (and, thus, our observable). In light of the fact that a Gaussian is completely determined by its mean and variance, any moment of the emission time $\hat{\tau}(s)$ can be computed once we know its mean μ and variance σ^2. Since by construction the mean of the Fock vacuum is zero, we have for the mean and the variance of the emission time

$$\mu = \langle 0|\tilde{\tau}(s)|0\rangle = \tau_{cl}(s)(\langle 0|1|0\rangle + \langle 0|r(\hat{h})|0\rangle + \mathcal{O}(h^2)) = \tau_{cl}(s) + \mathcal{O}(h^2), \tag{4.1}$$

$$\sigma^2 = \langle 0|\tilde{\tau}(s)^2|0\rangle - \langle 0|\tilde{\tau}(s)|0\rangle^2 \tag{4.2}$$

$$= \tau_{cl}^2(s)(1 + 0 + \langle 0|r(\hat{h})^2|0\rangle + \langle 0|r_2(\hat{h})|0\rangle - 1 + \mathcal{O}(h^3)) \sim \tau_{cl}^2(s)\langle 0|r(\hat{h})^2|0\rangle, \tag{4.3}$$

where we expanded the emission time up to linear order in the gravitational field as defined in eq. (3.4), i.e., $\tilde{\tau}(s) = e^{\tilde{r}(\hat{h})}\tau_{cl}(s) = \tau_{cl}(s)(1 + r(\hat{h}) + r_2(\hat{h}) + \mathcal{O}(h^3))$. It should be noted that this expansion breaks the Lorentzian signature. This can happen already at the classical level when the perturbations in the gravitational field are large. However, classically one can restrict these perturbations to be small and one can keep the Lorentzian signature, whereas quantum mechanically the perturbations are arbitrary. Therefore, at this point, we are not allowed to probe the causal structure of spacetime non-perturbatively anymore. A resolution to this may be an improved perturbation technique that keeps the Lorentzian signature. This could potentially be done using the Magnus expansion and may be worth investigation [8]. Another important point is that we neglected the term $r_2(\hat{h})$. This is yet another simplification and should be addressed in the future.

From the expression in eq. (4.3), we see that we are left calculating the first order corrections to the variance: $r(\hat{h})^2$. This immediately presents a problem, since all terms contain

$\langle \hat{h}(x)\hat{h}(y)\rangle \sim \frac{1}{(x-y)^2}$ which explodes for $x \longrightarrow y$. Fortunately, as a guiding analogy, we can look at a comparable situation that occurs in QED, where if we were to calculate the expectation value of the electric field at a single spacetime point squared, i.e., $\langle E(x)^2\rangle$, we would find out that it diverges. However, any realistic measurement that is carried out by a detector will have some finite spatial and temporal resolution. No detector is able to measure the electric field at one single spacetime point. Thus, we must not evaluate the integral at one single spacetime point but at a small region of spacetime, that is, we need to smear the result. If this smearing is carried out we find that the result is finite and represents the vacuum noise in a detector with a certain sensitivity profile (related to how the smearing is performed). We will use this regularization method and smear our results as well. We replace our gravitational field by

$$\hat{h}(x) \longrightarrow \tilde{h}(x) = \int \mathrm{d}z\, \hat{h}(x-z)\, g(z),$$

where $g(z)$ is the smearing function and can be interpreted as the detector sensitivity profile. Incontestably, we would like to make as little assumptions as possible about the smearing function, since we would like our final result to be independent of our choice of smearing. However, to make calculations possible, at this stage, we take $\tilde{g}_u(z) \sim g(z_\perp^2)\delta(z\cdot u)$, where $z = -(u\cdot z)u + z_\perp$. This is illustrated in fig. 4.1. Unfortunately, this choice of smearing breaks Lorentz symmetry. Up to this point the entire calculation was Lorentz invariant. Other choices of smearing may be addressed in the future.

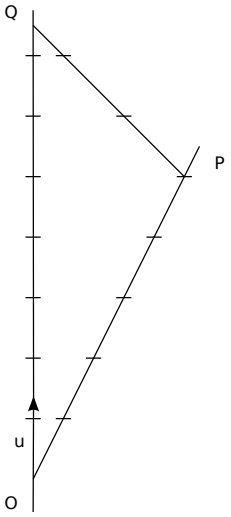

Figure 4.1: Illustration of choice of smearing: all spacetime intervals are smeared in the plane orthogonal to u and the smearing is rotationally symmetric within this plane.

The smeared first order correction to the variance is denoted by $\langle \tilde{r}^2\rangle$. Similar notation as described at the end of ch. 3.3 still applies, that is,

$$r \longrightarrow \tilde{r} = r^x \tilde{h}_x = \sum_{|K|mX} r^{Kij}_{|K|mX} \int^{(n)} \mathrm{d}z \nabla_K \tilde{h}_{ij}(z).$$

The first order correction in the gravitational field to the variance is then

$$\begin{aligned}
\langle \tilde{r}^2\rangle &= \frac{1}{2}\langle\{\tilde{r},\tilde{r}\}\rangle \\
&= \frac{1}{2}\sum_{|K|mX}\sum_{|L|nY} r^{Kij}_{|K|mX} r^{Lkl}_{|L|nY} \int \mathrm{d}x \int \mathrm{d}y\, \nabla_K \tilde{g}_u(x) \nabla_L \tilde{g}_u(y) \times \\
&\qquad \int_X^{(m)} \mathrm{d}x' \int_Y^{(n)} \mathrm{d}y'\, \langle\{\hat{h}_{(ij)}(x'-x), \hat{h}_{(kl)}(y'-y)\}\rangle \\
&= \frac{l_P^2}{2\pi}\sum_{|K|mX}\sum_{|L|nY} r^{Kij}_{|K|mX}\, \eta_{ij,kl}\, r^{Lkl}_{|L|nY} \int \mathrm{d}x \int \mathrm{d}y\, \nabla_K \tilde{g}_u(x) \nabla_L \tilde{g}_u(y) \times \\
&\qquad \int_{X-x}^{(m)} \mathrm{d}x' \int_{Y-y}^{(n)} \mathrm{d}y'\, P\frac{1}{[y'-x']^2} \\
&= \frac{l_P^2}{2\pi}\sum_{|K|mX}\sum_{|L|nY} r^{Kij}_{|K|mX}\, \eta_{ij,kl}\, r^{Lkl}_{|L|nY} \int \mathrm{d}x \int \mathrm{d}y\, \nabla_K \tilde{g}_u(x) \nabla_L \tilde{g}_u(y) I^{mn}(X-x; Y-y) \\
&= \frac{l_P^2}{2\pi}\sum_{|K|mX}\sum_{|L|nY} r^{Kij}_{|K|mX}\, \eta_{ij,kl}\, r^{Lkl}_{|L|nY} \int \mathrm{d}x \int \mathrm{d}y\, \nabla_K \tilde{g}_u(x) \nabla_L \tilde{g}_u(y) I^{mn}(X; Y+x-y)
\end{aligned}$$

$$= \frac{l_P^2}{2\pi} \sum_{|K|mX} \sum_{|L|nY} r^{Kij}_{|K|mX}\, \eta_{ij,kl}\, r^{Lkl}_{|L|nY} \int \mathrm{d}z \int \mathrm{d}y\, \nabla_K \tilde{g}_u(z+y) \nabla_L \tilde{g}_u(y) I^{mn}(X; Y+z)$$

$$= \frac{l_P^2}{2\pi} \sum_{|K|mX} \sum_{|L|nY} (-)^{|L|} r^{Kij}_{|K|mX}\, \eta_{ij,kl}\, r^{Lkl}_{|L|nY} \int \mathrm{d}z\, I^{mn}(X; Y+z) \int \mathrm{d}y\, \nabla_{K\cup L} \tilde{g}_u(z+y) \tilde{g}_u(y)$$

$$= \frac{l_P^2}{2\pi} \sum_{|K|mX} \sum_{|L|nY} (-)^{|L|} r^{Kij}_{|K|mX}\, \eta_{ij,kl}\, r^{Lkl}_{|L|nY} \int \mathrm{d}z\, I^{mn}(X; Y+z) \nabla_{K\cup L} g_u(z)$$

$$= \frac{l_P^2}{2\pi} \sum_{|K|mX} \sum_{|L|nY} (-)^{|L|} r^{Kij}_{|K|mX}\, \eta_{ij,kl}\, r^{Lkl}_{|L|nY} \tilde{I}^{mn}_{K\cup L}(X; Y),$$

where in the first line I used that $\langle\{h_{ij}(x), h_{kl}(y)\}\rangle = \eta_{ij,kl}\, \frac{\ell_p^2}{\pi} P\left[\frac{1}{(x-y)^2}\right]$ (for a detailed derivation, see app. B.3, note that the result in there differs by a factor 4 due to eq.(3.2)). The last expression does not appear to be symmetric under the interchange of the K and L multi-indices. In fact, the extra $(-)^{|L|}$ factor symmetrizes the interchange property $\tilde{I}^{mn}_{K\cup L}(X;Y) = (-)^{|K|+|L|} \tilde{I}^{nm}_{L\cup K}(Y;X)$. Furthermore, the following definitions were used

$$I^{mn}(X;Y) = \int_X^{(m)} \mathrm{d}s \int_Y^{(n)} \mathrm{d}t\, P \frac{1}{[x(s)-y(t)]^2} \tag{4.4}$$

$$\tilde{I}^{mn}_K(X;Y) = \int \mathrm{d}z\, I^{mn}(X; Y+z) \nabla_K g_u(z) \tag{4.5}$$

$$g_u(z) = \int \mathrm{d}z'\, \tilde{g}_u(z+z') \tilde{g}_u(z') = \int \mathrm{d}z'\, \tilde{g}_u(z-z') \tilde{g}_u(-z') \tag{4.6}$$

$$= \int \mathrm{d}z'\, \tilde{g}_u(z-z') \tilde{g}_u(z') = (\tilde{g}_u * \tilde{g}_u)(z) \tag{4.7}$$

where in eq. (4.7) the start $*$ indicates convolution and the relation $\tilde{g}_u(-z') = \tilde{g}_u(z')$ was used to go from eq. (4.6) to eq. (4.7). The convolved smearing function should have the same properties as the original smearing function: it is supported in the hyperplane perpendicular to u that passes through the origin. Within this plane, the function has compact support and depends only on $z_\perp^2$, i.e., it is rotationally symmetric in this plane. Furthermore, note the translation invariance $I^{mn}(X+z; Y+z) = I^{mn}(X;Y)$. The explicit calculation of $\langle \tilde{r}^2 \rangle$ is carried out in the next chapter.[1]

4.3 Previous work

In the field of quantum gravity, not much research has focused on calculating observables without presupposing any new fundamental physics in addition to the quantization of the metric field. Previous works that are most similar to this thesis are [10, 11, 12, 13, 14, 15]. The work in [10] calculates lengths of spacelike line segments in linearized quantum gravity. A drawback of this work is that these length operators are gauge variant and hence unphysical. Gauge invariant quantities were obtained by considering the perimeter of piecewise linear, closed curves.

[1] It should be remarked that the effects studied are solely due to quantum fluctuations in the gravitational field. Clearly, there are many other effects that contribute to a change in the variance of the emission time, for instance, possible jets caused by the probe at the ejection point and the non-zero mass of the lab and the probe. Quantum and classical effects are distinguishable as quantum effects are expected to only contribute at order $\hbar$ whereas any non-quantum effects are expected to be much larger. Quantum fluctuations in time measurements may come from various sources. Quantum but *non-quantum gravitational* contributions to the fluctuation of these measurements have been studied extensively. For example, Salecker and Wigner found that quantum limitations on the precision of clocks are of the order $\hbar/\epsilon$ where ϵ is the energy spread of a pointer indicating the passing of time [9]. However, these processes are not of interest to us and we focus only on the *quantum gravitational* influence on the time delay observable.

However, a clear physical interpretation of these observables was not given. Our calculation, on the other hand, is completely gauge-independent and our observable has a clear physical interpretation, stemming from the associated measurement protocol. The work by Ford and his collaborators in [11, 12, 13, 14] calculates light-cone fluctuations in linearized quantum gravity. There are two main distinctions between their work and this thesis. First, to regularize the divergences Ford et al. computed the effects of quantum fluctuations for various scenarios (finite temperature state, squeezed vacuum, extra compactified dimensions) and subtracted the divergent Minkowski, Poincaré invariant vacuum result. Consequently, these regularization procedures all ignore quantum contributions from Minkowski space itself, whereas we have included these in our calculation. Second, their results are restricted to specific experimental set-up they considered. As will be discussed in more detail in ch. 7, the calculation carried out in this thesis is flexible to the experimental set-up and can be easily extended to an arbitrary polygon with time-like and null-like edges confined to a plane. The research in [15] also aims at defining and evaluating observables in quantum gravity given by n-point functions determined by geodesic separation and parallel transport (so-called Mandelstam covariants). The main difference with this thesis is (again) the method of regularization. In their paper, dimensional regularization is used whereas we have chosen a physically more intuitive regularization procedure. Moreover, the physical motivation proposed in [15] (elimination of ultraviolet divergences) is very different from ours, whose emphasis is on a procedure to construct meaningful physical observables in gravity. On the other hand, some of the multiple physical motivations proposed in the more detailed work [16] are very close to ours.

Chapter 5

Explicit calculation

As shown in the previous chapter, we are left to evaluate

$$\langle \tilde{r}^2 \rangle = \frac{l_P^2}{2\pi} \sum_{|K|mX} \sum_{|L|nY} (-)^{|L|} r^{Kij}_{|K|mX}\, \eta_{ij,kl}\, r^{Lkl}_{|L|nY} \tilde{I}^{mn}_{K\cup L}(X;Y). \tag{5.1}$$

The bulk of the work lies in evaluating the $\tilde{I}^{mn}_{K\cup L}(X;Y)$ integral. Since for each term in $\tilde{r}^2$ we have such an integral, and $\tilde{r}$ consists of ten terms, we have to evaluate $\frac{1}{2}\cdot 10\cdot 11 = 55$ such integrals. Additionally, each integral contains $6-8$ one-dimensional integrals, which makes a total of integrals ~ 400 one-dimensional integrals. This is not the entire story yet, looking closer at the integrals one notices that the singularity structure changes depending on whether the line segments along which the integral needs to be evaluated are either time-like or null-like and parallel or non-parallel. Together with some additional technical details to be discussed, this results in ten different singularity structures. Therefore, no single master equation can be applied and we resort to hybrid numerical-analytical calculations automated using the computer algebra software *Mathematica 8.0*. In this chapter, the evaluation of the integral $\tilde{I}^{mn}_{K\cup L}(X;Y)$ and $\langle \tilde{r}^2 \rangle$ is discussed. First, the general set-up of the calculation of this integral is outlined by splitting the computation into two parts. These two parts are discussed next. Lastly, an overview of the entire procedure for computing $\langle \tilde{r}^2 \rangle$ is given.

5.1 General set-up of calculation

The integral in eq. (5.1) is completely determined by the number of derivatives $|K|$ on the smearing function ($|K| = 0, 1, 2$) (with K being the multi-index that collects all the corresponding indices), the number of iterated integrals along the X and Y segments denoted by m and n (where $m = 0, 1$ and similarly for n) and the line segments along which the integrals need to be evaluated. We decompose $z = -(u\cdot z)z + (\hat{u}\cdot z)\hat{u} + w$, where $\hat{u}$ is a space-like unit vector, taken to be $\hat{u}^i = (0, 1, 0, 0)$ (hence $u\cdot\hat{u} = 0$) and w is orthogonal to the $(u, \hat{u})-$plane. We parametrize z as $z = \left(-u\cdot z, \hat{u}\cdot z, w^1, w^2\right) = (T, R\cos\theta, R\sin\theta\cos\phi, R\sin\theta\sin\phi)$ and write the four dimensional integral over the spacetime separation in $\tilde{I}^{mn}_{K\cup L}(X;Y)$ as

$$\begin{aligned}\int \mathrm{d}^4 z &= \int \mathrm{d}(u\cdot z) \int \mathrm{d}(\hat{u}\cdot z) \int \mathrm{d}^2 w \\ &= \int_{-\infty}^{\infty} \mathrm{d}T \int_{-R}^{R} \mathrm{d}c \int_0^{2\pi} \mathrm{d}\phi \int_0^{\infty} \mathrm{d}R\, R,\end{aligned}$$

where we defined $c = R\cos\theta$ and $w^2 = R^2 - c^2$.

As discussed in the previous chapter, the smearing function is set to $g_u(z) = g(z_\perp^2)\delta(u \cdot z)$. The smearing function with any number of derivatives can be written compactly as

$$\nabla_k \, g_u(z) = \sum_{T,d,\gamma,p} T_k \delta^{(d)}(-T) \, g^{(\gamma)}(R^2) \, R^p \; P_{T,\gamma,p,d}(c), \tag{5.2}$$

where k is a multi-index, the coefficients $P_{T,\gamma,p,d}$ depend only on c and T_k is a certain tensor basis consisting of symmetrized products of u, $\hat{u}$ and $\delta_\perp = \eta + uu$. The coefficients are non-zero only when the indices satisfy the homogeneity constraint $d + 2\gamma - p = |k|$. For the integrals we are considering, the maximal number of derivatives on the smearing function is two, so T_k is either $\{1\}$ for zeroth derivatives, $\{u, \hat{u}\}$ for first derivatives, or $\{uu, \hat{u}\hat{u}, u\hat{u} + \hat{u}u, \delta_\perp\}$ for second derivatives. The maximal power of c in $P_{T,\gamma,p,d}$ is also two. For later reference, the exact expression for all the required derivatives of the smearing function can be found in tab. 5.1. Since the smearing function is independent of the direction of w and since $I^{mn}(X;Y)$ also only depends on w^2, $g_u(z)$ and its derivatives can be independently averaged over the directions of w. This averaging over the directions of w is indicated in the table by $\to$ and the averaged result in the new variables R and T by $\Rightarrow$.

$g_u(z)$	$= g(z_\perp^2)\delta(u \cdot z)$
$\nabla g_u(z)$	$= ug(z_\perp^2)\delta'(u \cdot z) + 2z_\perp g'(z_\perp^2)\delta(u \cdot z)$
	$= ug(z_\perp^2)\delta'(u \cdot z) + 2[(\hat{u} \cdot z)\hat{u} + w]g'(z_\perp^2)\delta(u \cdot z)$
	$\to ug(z_\perp^2)\delta'(u \cdot z) + 2\hat{u}(\hat{u} \cdot z)g'(z_\perp^2)\delta(u \cdot z)$
	$\Rightarrow ug(R^2)\delta'(-T) + 2\hat{u}cg'(R^2)\delta(-T)$
$\nabla\nabla g_u(z)$	$= uug(z_\perp^2)\delta''(u \cdot z) + 2(z_\perp u + uz_\perp)g'(z_\perp^2)\delta'(u \cdot z)$
	$\quad +[2\delta_\perp g'(z_\perp^2) + 4z_\perp z_\perp g''(z_\perp^2)]\delta(u \cdot z)$
	$= uug(z_\perp^2)\delta''(u \cdot z) + 2[(u\hat{u} + \hat{u}u)(\hat{u} \cdot z) + (wu + uw)]g'(z_\perp^2)\delta'(u \cdot z)$
	$\quad +[2\delta_\perp g'(z_\perp^2) + 4(\hat{u}\hat{u}(\hat{u} \cdot z)^2 + (\hat{u}w + w\hat{u})(\hat{u} \cdot z) + ww)g''(z_\perp^2)]\delta(u \cdot z)$
	$\to uug(z_\perp^2)\delta''(u \cdot z) + 2(\hat{u}u + u\hat{u})(\hat{u} \cdot z)g'(z_\perp^2)\delta'(u \cdot z)$
	$\quad + \left[2\delta_\perp g'(z_\perp^2) + 4\left(\hat{u}\hat{u}(\hat{u} \cdot z)^2 + \frac{1}{2}(\delta_\perp - \hat{u}\hat{u})w^2\right) g''(z_\perp^2)\right] \delta(u \cdot z)$
	$\Rightarrow uug(R^2)\delta''(-T) + 2(\hat{u}u + u\hat{u})cg'(R^2)\delta'(-T)$
	$\quad + \left[2\delta_\perp g'(R^2) + \left(4\hat{u}\hat{u}c^2 + 2(\delta_\perp - \hat{u}\hat{u})(R^2 - c^2)\right) g''(R^2)\right] \delta(-T)$

Table 5.1: Smearing function with zero, one or two derivatives. Primes denote derivatives with respect to the argument of the corresponding function. The $\to$ indicates averaging over the directions of w in z-coordinates. The $\Rightarrow$ signifies the averaged result in (R, T)-coordinates.

The averaging procedure for w is fairly straightforward. For symmetry reasons, all terms that are odd in w when averaged give zero. Thus, we solely need to consider terms that are even in w. From tab. 5.1, we observe that only the following averaging is needed

$$\int_{|w|=1} \mathrm{d}^2 w \, w_i w_j,$$

where for clearness of notation we restricted $|w| = 1$. The integrated result should be symmetric in the $(i, j)-$indices. In addition, it needs to be invariant under simultaneous rotation of w_i and w_j. The only tensor that allows this is $\delta_{ij}^\perp = \eta_{ij} + u_i u_j$ in combination with $\hat{u}_i \hat{u}_j$. Thus,

$$\int_{|w|=1} \mathrm{d}^2 w \, w_i w_j = C \left(\delta_{ij}^\perp - \hat{u}_i \hat{u}_j\right),$$

where C is an unknown constant that needs to be determined. This is done by contracting both sides of the equation by $(\delta^\perp)^{ij}$. Making use of the following identities

$$(\delta^\perp)^{ij}\delta_{ij}^\perp = 3,$$
$$(\delta^\perp)^{ij}\hat{u}_i\hat{u}_j = 1,$$

the contraction yields

$$\int_{|w|=1} \mathrm{d}^2 w\, w^2 = 2C \Longrightarrow C = \frac{1}{2}\, 2\pi.$$

Therefore, the average over $w_i w_j$ is given by

$$\frac{1}{2\pi} \int \mathrm{d}^2 w\, w_i w_j = \frac{1}{2}(R^2 - c^2)\left(\delta_{ij}^{\perp} - \hat{u}_i \hat{u}_j\right),$$

where we took into account that $|w| \neq 1$, but in fact $w^2 = R^2 - c^2$.

Substitution of eq.(5.2) into eq.(4.5) gives

$$\tilde{I}_k^{mn}(X;Y) = \sum_{T,d,\gamma,n'} T_k \underbrace{\int_0^{2\pi} \mathrm{d}\phi \int_{-\infty}^{\infty} \mathrm{d}T \delta^{(d)}(-T) \int_0^{\infty} \mathrm{d}R\, R^p g^{(\gamma)}(R^2) \times}_{\text{part II}} \underbrace{\int_X^{(m)} \mathrm{d}s \int_Y^{(n)} \mathrm{d}t \int_{-R}^{R} \mathrm{d}c P \frac{P_{T,\gamma,p,d}(c)}{(y(t) - x(s) + z)^2}}_{\text{part I}} \tag{5.3}$$

Since the smearing function depends only on R and T, the evaluation of this integral can be broken down into two parts: generating tables (indicated by part I) after which the remaining smearing needs to be performed (indicated by part II). Before starting the calculation, it should be noted that since $g(R^2)$ is expected to be concentrated about $R = 0$, we only need to expand the integrand as a series in $R^n \ln^m R$ and keep the terms with the smallest n that do not vanish after integration. Thus, we do not need to carry out the calculations in full generality, but we can significantly simplify the calculations by Taylor expanding the results at an early stage (and thereby enhance the processing time of the computer).

5.2 Generating tables

The integral that we are concerned with in this chapter is part I of eq. (5.3), i.e.,

$$\int_X^{(m)} \mathrm{d}s \int_Y^{(n)} \mathrm{d}t \int_{-R}^{R} \mathrm{d}c\, P \frac{c^l}{z(s,t,c)^2},$$

where $P_{T,\gamma,p,d}(c)$ is replaced by c^l with $l \in \{0,1,2\}$ and we can write the denominator as $z(s,t,c)^2 = [y(t) - x(s) + Tu + c\hat{u}]^2 + (R^2 - c^2)$, where the appearance of T, c and R is a result of the smearing previously displayed by z. When we confine the line segments and the displacement to the $(u,\hat{u})-$plane, this denominator can be rewritten

$$\begin{aligned} z(s,t,c)^2 &= [y(t) - x(s) + Tu]^2 + 2c[y(t) - x(s) + Tu] \cdot \hat{u} + c^2 + (R^2 - c^2) \\ &= -z_0^2 + z_1^2 + 2cz_1 + c^2 + (R^2 - c^2) \end{aligned}$$

where $z_0 = -z \cdot u$ and $z_1 = z \cdot \hat{u}$ when z is shifted only temporally, i.e., $z = x - y + Tu$. In this form, we see that the denominator depends only linearly on c, which makes integration with respect to c rather straightforward. After the c-integration, upon substituting the integral endpoints $c = \pm R$ and rearranging the denominator once more using the following definitions

$$v_{\pm} = v \cdot (\hat{u} \pm u), \tag{5.4}$$

$$z_{c\pm} = c + z_1 \mp z_0 = c + z_{\pm}, \tag{5.5}$$

we get

$$z(s,t,c = \pm R)^2 = -z_0^2 + (z_1 + c)^2 = (c + z_1 - z_0)(c + z_1 + z_0) = z_{c+} z_{c-}.$$

Performing the integration over c in terms of these new variables $z_{c\pm}$ and z_1 yields

$$\begin{aligned}\int_{-R}^{R} \mathrm{d}c \frac{c^l}{-z_0^2+z_1^2+2cz_1+R^2} &= \sum_{c=\pm R} \pm \left(2\bar{P}_1(c,z_0;z_1) + P_2(z_{c\pm};z_1)[\ln|z_{c+}| + \ln|z_{c-}|]\right) \\ &= \sum_{c=\pm R} \pm \sum_{\pm} \left(P_1(c,z_{c\pm};z_1) + P_2(z_{c\pm};z_1)\ln|z_{c\pm}|\right),\end{aligned}$$

where the $\pm$-symbol following the summation over c matches the sign in this summation. $\bar{P}_1$ and P_1, P_2 are polynomials in the arguments before the semi-colon and Laurent polynomial in the arguments after the semi-colon. The first two are related by

$$P_1(c,z_{c\pm};z_1) = \bar{P}_1(c,\mp(z_{c\pm}-z_1-c);z_1).$$

Since z_1 appears as a Laurent polynomial, the individual summmands in the result of the c integral may have poles for $z_1 = 0$. However, the integral we started with was regular for $z_1 = 0$ and thus these singularities need to vanish in the final result. This will serve as a check on our calculations.

Integration along s and t

The integration over c has been carried out and we are left with the single and iterated integrals over s and t. However, rather than first parametrizing the spacetime interval over which we need to integrate and subsequently integrating over it, we perform a change of variables to the $(u,\hat{u})-$plane, which is spanned by the worldlines of the lab and the probe and perform the integration there. This change of variables is illustrated for two single integrals in fig. 5.1.

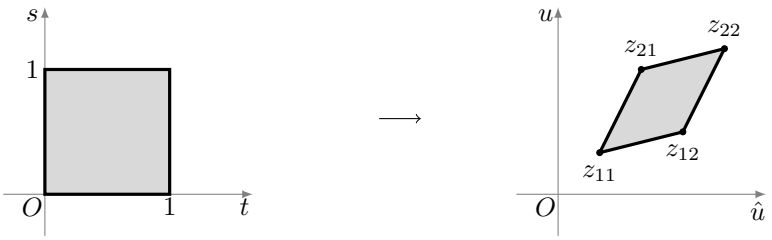

Figure 5.1: Illustration of the change of variables from (s,t) to the $(u,\hat{u})-$plane.

The sides of the parallelogram are parametrized by the standard affine parametrization

$$\begin{aligned} y(t) &= y_1 + (y_2-y_1)t && \text{with} \quad y(0)=y_1,\ y(1)=y_2 \\ x(s) &= x_1 + (x_2-x_1)s && \text{with} \quad x(0)=x_1,\ x(1)=x_2 \end{aligned}$$

and the vertices of the parallelogram are given by

$$z_{ij} = y_j - x_i.$$

The normalized, iterated integrals are treated similarly as the single integrals, after they are reduced to single integrals using Cauchy's formula for iterated integrals

$$\int_X^{(m)} \mathrm{d}s = \int_X \mathrm{d}s\, \frac{(1-s)^m}{m!},$$

where the integration range is from 0 to 1, and similarly for t-integrals. Thus, after this reduction procedure and change of variables the integrands are functions of $s, t, z_{c\pm}$ and z_1, which we need to integrate over $z_{c\pm}$ and z_1.

There are two different situations to consider: integration along non-parallel and parallel line segments. This is because in the non-parallel situation $z_{c\pm}$ and z_1 are independent variables and can be used as alternative integration variables. In contrast, for parallel line segments this is not true. Hence, we will discuss both cases separately: the non-parallel situation first and the parallel one next.

Non-parallel line segments

When the line segments X and Y are non-parallel, we can make a change of variables from (s,t) to $(z_{c\pm}, z_1)$. We let $z = z_{11}$ when $s = t = 0$. The relation between the old (s,t) and new $(z_{c\pm}, z_1)$ variables is

$$s = \frac{y \wedge (z - z_{11})}{x \wedge y} \qquad \text{and} \qquad t = \frac{x \wedge (z - z_{11})}{x \wedge y},$$

where we defined

$$v \wedge w = -(v \cdot u)(w \cdot \hat{u}) + (w \cdot u)(v \cdot \hat{u})$$

from which the following identity follows

$$v \wedge w = \pm[(v \cdot \hat{u}) w_{\pm} - (w \cdot \hat{u}) v_{\pm}].$$

The differentials are related by

$$\mathrm{d}s \wedge \mathrm{d}t = -\frac{\mathrm{d}z_0 \wedge \mathrm{d}z_1}{x \wedge y} = \pm \frac{\mathrm{d}z_{c\pm} \wedge \mathrm{d}z_1}{x \wedge y}.$$

So the integral that we are interested in now looks like

$$\int^{(m)} \mathrm{d}s \int^{(n)} \mathrm{d}t \, (P_1(c, z_{c\pm}; z_1) + P_2(z_{c\pm}; z_1) \ln |z_{c\pm}|) = \tag{5.6}$$

$$\int_0^1 \mathrm{d}s \int_0^1 \mathrm{d}t \frac{(1-s)^m}{m!} \frac{(1-t)^n}{n!} \, (P_1(c, z_{c\pm}; z_1) + P_2(z_{c\pm}; z_1) \ln |z_{c\pm}|) = \tag{5.7}$$

$$\pm \int \int \frac{\left(1 - \frac{y \wedge (z - z_{11})}{x \wedge y}\right)^m}{m!} \frac{\left(1 - \frac{x \wedge (z - z_{11})}{x \wedge y}\right)^n}{n!} \, (P_1(c, z_{c\pm}; z_1) + P_2(z_{c\pm}; z_1) \ln |z_{c\pm}|) \, \frac{\mathrm{d}z_{c\pm} \wedge \mathrm{d}z_1}{x \wedge y}. \tag{5.8}$$

Since any 2-form is closed (being top-dimensional), by the Poincaré lemma, it is also exact, i.e. we can write the differentials in eq. (5.8) as $\mathrm{d}Q$ where Q is some 1-form. Then by Stokes' theorem, which states that

$$\int_M \mathrm{d}\omega = \int_{\partial M} \omega,$$

where M is an oriented n-dimensional smooth manifold, ∂M its boundary with the induced orientation and ω an $(n-1)-$form with compact support on M, we can reduce the integral in eq. (5.8) from an integral over the interior to an integral over the boundary of the parallelogram. The boundary of the st-integration domain is $(0,0) \xrightarrow{s} (1,0) \xrightarrow{t} (1,1) \xrightarrow{-s} (0,1) \xrightarrow{-t} (0,0)$. In terms of the z-integration domain, it becomes $z_{11} \xrightarrow{-x} z_{21} \xrightarrow{y} z_{22} \xrightarrow{x} z_{12} \xrightarrow{-y} z_{11}$. We can formalize this procedure as follows. We are to integrate an expression of the form $P = dQ$ where Q is some 1-form. If we pull Q back to any line, then Q is also top-dimensional and therefore closed. Thus, we can write $Q_x = dL$ where the subscript indicates that Q is restricted to the

line x and L is a 0-form. This gives

$$\int_{X\wedge Y} P = \int_{X\wedge Y} \mathrm{d}Q \tag{5.9}$$

$$= \int_{z_{11}\xrightarrow{-x}z_{21}} Q_{-x} + \int_{z_{21}\xrightarrow{y}z_{22}} Q_y + \int_{z_{22}\xrightarrow{x}z_{12}} Q_x + \int_{z_{12}\xrightarrow{-y}z_{11}} Q_{-y} \tag{5.10}$$

$$= [L_x(z_{21}) - L_x(z_{11})] + [L_y(z_{22}) - L_y(z_{21})] + [L_x(z_{12}) - L_x(z_{22})] + [L_y(z_{11}) - L_y(z_{12})] \tag{5.11}$$

$$= \sum_{\mu,\nu=1,2} (-)^{\mu+\nu}[L_y(z_{\mu\nu}) - L_x(z_{\mu\nu})]. \tag{5.12}$$

Hence, by applying Stokes' theorem, we reduced the integral over the interior of the parallelogram to the edges, which amounts to a sum over the vertices. The subscripts $-x$ and x, as well as $-y$ and y, are not distinguished in the final formula, since the resulting expressions are identical in the calculations considered here.

Parallel line segments

When the line segments are parallel, it is no longer possible to construct an invertible transformation between (s,t) and (z_0,z_1). On the other hand, this failure indicates that we can write z_0, z_1, $z(s,t,c)^2$ or any function $F(z_0,z_1)$ as a function $F(\zeta(s,t))$ of some single affine-linear combination $\zeta(s,t)$ of s,t with non-zero constants $\zeta_s = \mathrm{d}\zeta/\mathrm{d}s$, $\zeta_t = \mathrm{d}\zeta/\mathrm{d}t$. Each s or t integral can then be converted into a ζ integral. The iterated integrals are now handled recursively. Denote $\zeta = \zeta(s,t)$, $\zeta^S = \zeta(0,t)$, $\zeta^T = \zeta(s,0)$ and $\zeta^{ST} = \zeta(0,0)$ and define

$$\begin{aligned} F_{m,n} =& \frac{F^{[m+n+2]}(\zeta)}{\zeta_s^{m+1}\zeta_t^{n+1}} + \sum_{k=0}^{m+n+2} p^S_{m,n;k}(s)\frac{F^{[k]}(\zeta^S)}{\zeta_t^{n+1}} \sum_{k=0}^{m+n+2} p^T_{m,n;k}(t)\frac{F^{[k]}(\zeta^T)}{\zeta_s^{m+1}} \\ &+ \sum_{k=0}^{m+n+2} p^{ST}_{m,n;k}(s,t)F^{[k]}(\zeta^{ST}), \end{aligned} \tag{5.13}$$

where

$$\begin{aligned} &\frac{\mathrm{d}}{\mathrm{d}\zeta}F^{[k+1]}(\zeta) = F^{[k]}(\zeta), \\ &F^{[0]}(\zeta) = F(\zeta), \\ &F_{-1,-1} = F(\zeta), \end{aligned}$$

with p's being polynomials in their arguments. The form of this expression is preserved under integrations with respect to s or t

$$\int_0 \mathrm{d}s\, F_{m,n} = F_{m+1,n} \quad \text{and} \quad \int_0 \mathrm{d}t\, F_{m,n} = F_{m,n+1}.$$

Setting $s = t = 1$ in $F_{m,n}$ yields $\tilde{I}_K^{mn}$ for a proper choice of $F(\zeta)$. Note that the integration constants are chosen such that $F_{m,n} = 0$ whenever either $s = 0$ or $t = 0$ for either $m \geq 0$ or $n \geq 0$. With the above initial conditions, the polynomial coefficients will satisfy the following

recurrence relations

$$
\begin{aligned}
p^S_{m+1,n;k}(s) &= \int_0 \mathrm{d}s\, p^S_{m,n;k}(s) - \frac{\delta_{k,m+1+n+2}}{\zeta_s^{m+2}},\\
p^S_{m,n+1;k}(s) &= p^S_{m,n;k-1}(s),\\
p^T_{m,n+1;k}(t) &= \int_0 \mathrm{d}t\, p^T_{m,n;k}(t) - \frac{\delta_{k,m+n+1+2}}{\zeta_t^{n+2}},\\
p^T_{m+1,n;k}(t) &= p^T_{m,n;k-1}(t),\\
p^{ST}_{m+1,n;k}(s,t) &= \int_0 \mathrm{d}s\, p^{ST}_{m,n;k}(s,t) - \frac{p^T_{m,n;k-1}(t)}{\zeta_s^{m+2}},\\
p^{ST}_{m,n+1;k}(s,t) &= \int_0 \mathrm{d}t\, p^{ST}_{m,n;k}(s,t) - \frac{p^S_{m,n;k-1}(s)}{\zeta_t^{n+2}}.
\end{aligned}
$$

The coefficients that are relevant for the integrals we are considering can be found in tab. 5.2.

		p	p^S	p^T	p^{ST}
$m=0,n=0$	$k=2$	$\frac{1}{\zeta_s\zeta_t}$	$-\frac{1}{\zeta_s\zeta_t}$	$-\frac{1}{\zeta_s\zeta_t}$	$\frac{1}{\zeta_s\zeta_t}$
$m=1,n=0$	$k=2$		$-\frac{s}{\zeta_s\zeta_t}$		$\frac{s}{\zeta_s\zeta_t}$
	$k=3$	$\frac{1}{\zeta_s^2\zeta_t}$	$-\frac{1}{\zeta_s^2\zeta_t}$	$-\frac{1}{\zeta_s^2\zeta_t}$	$\frac{1}{\zeta_s^2\zeta_t}$
$m=0,n=1$	$k=2$			$-\frac{t}{\zeta_s\zeta_t}$	$\frac{t}{\zeta_s\zeta_t}$
	$k=3$	$\frac{1}{\zeta_s\zeta_t^2}$	$-\frac{1}{\zeta_s\zeta_t^2}$	$-\frac{1}{\zeta_s\zeta_t^2}$	$\frac{1}{\zeta_s\zeta_t^2}$
$m=1,n=1$	$k=2$				$\frac{st}{\zeta_s\zeta_t}$
	$k=3$		$-\frac{s}{\zeta_s\zeta_t^2}$	$-\frac{t}{\zeta_s^2\zeta_t}$	$\frac{s\zeta_s+t\zeta_t}{\zeta_s^2\zeta_t^2}$
	$k=4$	$\frac{1}{\zeta_s^2\zeta_t^2}$	$-\frac{1}{\zeta_s^2\zeta_t^2}$	$-\frac{1}{\zeta_s^2\zeta_t^2}$	$\frac{1}{\zeta_s^2\zeta_t^2}$

Table 5.2: The polynomial coefficients for the parallel case for different values of m, n and k.

Thus, also for the parallel situation, we are left to evaluate one-dimensional integrals, in particular, integrals parametrized by $\zeta(s,t)$. The case that we are interested in will require $2, 3$ and maximally 4 iterated integrals. One can think of these integrals in a similar way as for the integrals in the non-parallel situation: the $\zeta(s,t)$ parametrizes the sides of the parallelogram and the four terms in eq. (5.13) correspond to the four edges of the parallelogram.

In sum, for both situations, non-parallel and parallel line segments, we are left to evaluate one-dimensional integrals along the sides of the parallelogram. Evaluation of these one-dimensional integrals is discussed next. We again need to consider two different situations: one in which the edge is completely in the direction of u and one in which the edge also has a $\hat{u}-$component. A different parametrization is needed for each case. However, in both cases, each side of the parallelogram is described by its starting point b and its tangent vector a, which runs from one vertex to the next. First the procedure for the latter situation, which corresponds to $a \cdot \hat{u} \neq 0$ is outlined and successively the situation in which the edge is entirely in the $u-$direction, that is, $a \cdot \hat{u} = 0$.

Parametrization of line segments

Case $a \cdot \hat{u} \neq 0$. When $a \cdot \hat{u} \neq 0$, we parametrize each edge by $z(\sigma) = z_0(\sigma)u + z_1(\sigma)\hat{u}$ with

$$
\begin{aligned}
z_0(\sigma) &= B_0 - C_0\sigma,\\
z_1(\sigma) &= \sigma.
\end{aligned}
$$

To relate the constants B_0 and C_0 to the geometry of the parallelogram, we look at the "velocity" of the edge

$$\frac{\mathrm{d}}{\mathrm{d}\sigma} z(\sigma) = Ka,$$

where K is an unknown constant. If we dot this equation with $-u$ and $\hat{u}$, we can compare this to the derivatives of z_0 and z_1 to determine C_0 in terms of the a and b vectors

$$\frac{-K(a\cdot u)}{K(a\cdot\hat{u})} = \frac{\frac{\mathrm{d}z_0(\sigma)}{\mathrm{d}\sigma}}{\frac{\mathrm{d}z_1(\sigma)}{\mathrm{d}\sigma}} = \frac{-C_0}{1} \Longrightarrow C_0 = \frac{a\cdot u}{a\cdot\hat{u}}.$$

From this expression, it is evident that $a\cdot\hat{u}$ cannot be equal to zero in this parametrization. However, this could be observed before, because we are integrating over z_1 which is in the $\hat{u}-$direction and hence we cannot have a term that is completely independent of $\hat{u}$.

To determine B_0 in terms of the a and b vectors, we look at the starting point of the edge which corresponds to $\sigma = 0$. At this point $z(\sigma=0) = b$, but also $z(\sigma=0) = z_0(0)u + z_1(0)\hat{u}$, which gives us two equations and one unknown:

$$a\wedge z|_{\sigma=0} = a\wedge b \qquad \Longrightarrow B_0 = -\frac{a\wedge b}{a\cdot\hat{u}}, \tag{5.14}$$

$$a\wedge z|_{\sigma=0} = B_0(a\wedge u) \tag{5.15}$$

where we used that $a\wedge u = (a\cdot\hat{u})\,(\hat{u}\wedge u) = -a\cdot\hat{u}$. After integration along the vertices, the begin and end point of each segment needs to be inserted (compare eq. (5.10)), therefore, we need to know the value of σ at each vertex. At each vertex $z = b \to z\cdot\hat{u} = b\cdot\hat{u}$ and in general we have $z\cdot\hat{u} = z_1 = \sigma$, therefore at each vertex $\sigma = b\cdot\hat{u}$.

The ($z_{c\pm}$,z_1) variables are related to these new variables as follows. We already know that $z_1 = \sigma$ and $z_{c\pm}$ is obtained by

$$\begin{aligned} z_{c\pm} &= c + z_1 \mp z_0 \\ &= c + \sigma \mp B_0 \pm C_0\sigma \\ &= B_{c\pm}\left(1 - C_{c\pm}\sigma\right), \end{aligned}$$

where we defined $B_{c\pm} = c \mp B_0$ and $C_{c\pm} = -\frac{1\pm C_0}{c\mp B_0}$. Hitherto, the shift in the u-direction by the smearing function is not explicitly taken into account. Fortunately, it can be simply reobtained by absorbing the shift in the b vector: $b\cdot u \to b\cdot u - T$. This gives

$$B_0 = -\frac{a\wedge b}{a\cdot\hat{u}} \longrightarrow -\frac{a\wedge b}{a\cdot\hat{u}} + T.$$

C_0 does not change as it does not contain b. Thus, taking the shift by the smearing into account, we have

$$\begin{aligned} B_{c\pm} &= \frac{(a\cdot\hat{u})(c\mp T) \pm a\wedge b}{a\cdot\hat{u}}, \\ C_{c\pm} &= -\frac{a_\pm}{a\cdot\hat{u}(c\mp T) \pm a\wedge b}. \end{aligned}$$

For the parallel case, we identify $\zeta = \sigma$. The constants ζ_s and ζ_t can also be related to this set-up by $\zeta_s = -x\cdot\hat{u}$ and $\zeta_t = y\cdot\hat{u}$.

Case $a\cdot\hat{u} = 0$. The second situation is when $a\cdot\hat{u} = 0$ for which a different parametrization of the edges is needed. This is simply done by reversing the role of z_0 and z_1

$$\begin{aligned} z_0 &= \sigma, \\ z_1 &= B_0 - C_0\sigma. \end{aligned}$$

Applying the same procedure as for $a \cdot \hat{u} \neq 0$, we obtain that in this parametrization $z_{c\pm} = B_{c\pm}(1 - C_{c\pm}\sigma)$ remains the same, but the constants $B_{c\pm}$ and $C_{c\pm}$ change

$$B_0 = b \cdot \hat{u} \qquad B_{c\pm} = c + b \cdot \hat{u}$$
$$C_0 = 0 \qquad C_{c\pm} = \frac{\pm 1}{c + b \cdot \hat{u}}$$

and at the starting point of each edge $\sigma = -b \cdot u$. When the shift due to smearing is taken into account, $B_{c\pm}$ and $C_{c\pm}$ are not altered. In contrast, at each edge σ is shifted to $\sigma \to -b \cdot u + T$. In the parallel case, again, we identify $\zeta = \sigma$. The constants ζ_s and ζ_t in this set-up are

$$\zeta_s = x \cdot u,$$
$$\zeta_t = -y \cdot u.$$

So in the non-parallel case using these new variables we have

$$\begin{aligned}
&\int \mathrm{d}z_{c\pm} \int \mathrm{d}z_1 \left(P_1 + P_2 \ln|z_{c\pm}|\right) \\
&= \int \mathrm{d}z_{c\pm} \int \mathrm{d}\sigma \left(P_3 + P_4 \ln|B_{c\pm}| + P_5 \ln|1 - C_{c\pm}\sigma|\right) \\
&= \left[\int \mathrm{d}\sigma (P_6 + P_7 \ln|B_{c\pm}| + P_8 \ln|1 - C_{c\pm}\sigma| + P_9 L\left(C_{c\pm}\sigma\right))\right]_{z_{c\pm}} \\
&= \left[\bar{P}_6 + \bar{P}_7 \ln|B_{c\pm}| + \bar{P}_8 \ln|1 - C_{c\pm}\sigma| + \bar{P}_9 L\left(C_{c\pm}\sigma\right)\right]_{z_{c\pm},\sigma},
\end{aligned} \tag{5.16}$$

where $L(x) = \mathrm{Re}\{\mathrm{Li}_2(x)\} = -\int_0^x \mathrm{d}t\, \frac{\ln|1-t|}{t}$, P_1, P_2 are as before (Laurent) polynomials in $z_{c\pm}$ and z_1 and the remaining P_i's and $\bar{P}_i$'s are (Laurent) polynomials in $B_{c\pm}, C_{c\pm}$ and σ. Going from the second to third line corresponds to going from our integral over the interior to the boundary (equivalently, from integrating over the 2-form to 1-form in eq. (5.10)). The integral in the third line is to be performed for each side along the parallelogram, resulting in a sum over $2 \cdot 2 \cdot 4$ cases, where the first two comes from inserting the $z_{c\pm}$ boundary conditions, the second two from the begin point and end point of each line segment and the four from each side of the parallelogram.

In the end, we are interested in obtaining an asymptotic expansion for small $R > 0$, with leading behavior of the form $R^n \ln^m R$ for $n \leq 0$ and m arbitrary, that is, we are interested in divergent terms. Looking at the resulting expression in eq. (5.16), we see that singularities arise when the arguments of the logarithms are either zero or $\pm\infty$, or when the argument of $L(x)$ is $\pm\infty$ or equal to one. The latter function, i.e. the real part of the dilog, can be rewritten using the following identities such that we can extract its logarithmic singularities

$$L(1/x) = -L(x) - \frac{1}{2}\ln^2|x| + \frac{\pi^2}{12} + \frac{x}{|x|}\frac{\pi^2}{4} \tag{5.17}$$

$$L(1-x) = -L(x) - \ln|1-x|\ln|x| + \frac{\pi^2}{6} \tag{5.18}$$

for real x [17]. When the argument of $L(x)$ is of the form R^n with $n < 0$ the first relation is applied, when the argument is of the form "one plus something small" the second identity is exploited. The singularities in the expression for $\langle \tilde{r}^2 \rangle$, see eq. (5.1), can ultimately be traced back to the light-cone and coincidence singularities of the graviton two-point function and are, as mentioned before, affected by the line segments along which is integrated. This information is now encoded in the a and b vectors of the edges of the parallelogram. For instance, when $a_\pm = 0$, the line segment is null-like and has a distinct singularity structure. Knowledge of the values for a and b vectors is thus important. However, this information becomes only relevant after all integrations have been carried out. Nonetheless, there is one important exception for

which we need to know the values of the a and b vectors: this is for integration along σ. This is an artifact of our computer algebra-software. *Mathematica 8.0* considers '$0 \ln 0$' as an infinite number, consequently, whenever such an expression appears the resulting answer it produces is bogus. Therefore, in these cases we need to tell *Mathematica 8.0* explicitly that this equals zero. The insertion of the determining features of the a and b vectors is discussed next. The resulting singularity structure is analyzed for the non-parallel and parallel case separately.

Singularity structures for non-parallel line segments

First note that when we consider non-parallel line segments and $a \cdot \hat{u} = 0$, the resulting integral is zero. This is due to the fact that the integrand is proportional to $\mathrm{d}z_1$ and an integral along a line where z_1 is constant automatically gives zero. Second, as mentioned before, we need to be careful when a term like '$0 \ln 0$' is present. This occurs in two situations: in the overall plus-summation in combination with $a_+ = 0$ and in the overall minus-summation in combination with $a_- = 0$. When this happens, the computer routine takes a slightly different route to avoid encountering '$0 \ln 0$'. The different cases are illustrated in the decision tree diagram in fig. 5.2, where the situation $a_\pm = 0$ with its corresponding overall sign is dubbed 'special' and the residual cases are categorized as 'generic'.

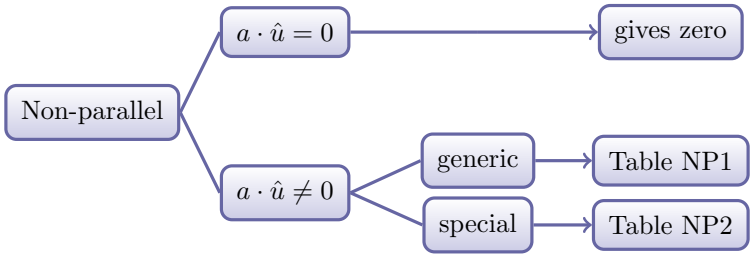

Figure 5.2: Decision tree summarizing the various cases for the non-parallel case.

As is indicated in the figure, the integrated results are stored in tables. Each table contains all integrated results of 'part I' for all relevant powers of c and all possible combinations of single and iterated integrals. To reduce calculation time, the integrated results are stored in expanded form in the variables R and T. The order of the expansion is not trivial. We want the final answer for $\langle \tilde{r}^2 \rangle$ to zeroth order in μ, which corresponds to a precision in R to second order (to be discussed in 'part II'). However, since we still need to take derivatives with respect to R and T due to the smearing function, the results in the table need to be expanded up to third, fourth or fifth order depending on whether the integrand in eq. (5.3) is proportional to c^0, c or c^2 respectively. [1]

Singularity structures for parallel line segments

The parallel situation is very similar to the non-parallel case. The only important difference is when $a \cdot \hat{u} = 0$, because now the resulting integral is not necessarily zero. Thus, this case is included when generating the tables. However, the situation in which $a \cdot \hat{u}$ and $a \cdot u$ are both equal to zero is not considered because it is not physically relevant for our experimental set-up as it corresponds to a line segment that is of zero size (a point). Furthermore, when generating the tables, we also treat the case when $z_1 = \sigma = b \cdot \hat{u} = 0$ separately. This is done by replacing σ in all terms by $b \cdot \hat{u}$, taking a Taylor series in $b \cdot \hat{u}$ and keeping only the zeroth order terms. The higher order terms will obviously vanish when taking $b \cdot \hat{u} \to 0$. The terms of lower order are more problematic, as they diverge when $b \cdot \hat{u} \to 0$. These terms, however, are checked to vanish

[1] The Taylor series in R and T are performed simultaneously using a standard trick. First, the variables R and T are replaced by ϵR and ϵT. Subsequently, the entire expression is Taylor expanded in ϵ to the desired order. Lastly, ϵ is set to 1 again.

in the final answer when all the summations are carried out. Thus, it is sufficient to just take the zeroth order term of the Taylor series in $b \cdot \hat{u}$ when $b \cdot \hat{u} = 0$. This case should have been treated separately for the non-parallel case as well. This was not done, however, as doing the expansion for symbolic expressions of the a and b vectors took too much computer capacity and a standard computer was not able to successfully finish this calculation. Therefore, for the non-parallel situation a different route is taken: we look up the relevant integrals, replace all the symbolic expressions with numerical values, except for $\sigma(= b \cdot \hat{u})$ and $b \cdot \hat{u}$, and subsequently perform the series expansion. Owing to the substitution of the numerical values the series expansion is now relatively fast. From this point onward, all cases are treated equally again. It should be noted that precalculating all series expansions and storing the results in tables as is done for the parallel case is the preferred method, because in principle looking up results in tables is much faster than performing a series expansion. This is illustrated by the fact that calculating 'part I' for parallel line segments with $b \cdot \hat{u} = 0$ is much faster than the same calculation for non-parallel line segments with $b \cdot \hat{u} = 0$.

The decision diagram for the parallel case is shown in fig. 5.3. As for the non-parallel situation, each table contains the results in Taylor expanded form for different powers of c and for single as well as iterated integrals.

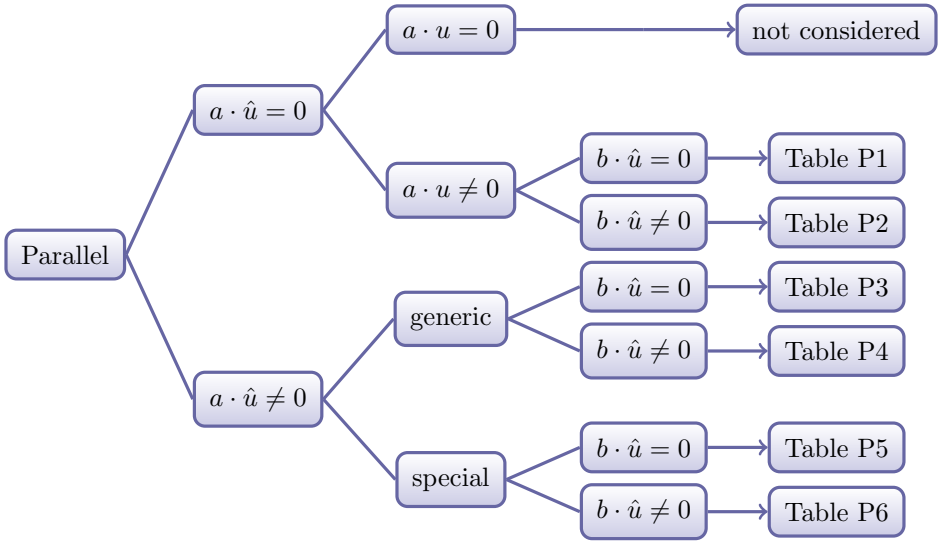

Figure 5.3: Decision tree summarizing procedure for the parallel case.

5.3 Remaining smearing

Part II of eq. (5.3) is to be performed next. This is done for each tensor basis element of the smearing function independently. The procedure is as follows.

1. First, the derivatives on the delta-function with argument T are moved onto the remaining part of the integrand using integration by parts.[2] After all derivatives on the delta-function have been removed, the T-integration is straightforwardly carried out by replacing $T \to 0$. Note that due to the appearance of $L(x)$ after integration and rewriting this term using eq. (5.17) or (5.18), $\mathrm{sgn}(R \pm T)$ terms may be part of the integrand. When derivatives are taken with respect to T, these terms give delta-functions and derivatives thereof again. However, these form no problem as the argument also contains R.

[2]There are no boundary terms, since the delta-function is a distribution which is defined not to have boundary terms.

2. Second, the derivatives on these delta-functions with argument R, when they appear, also need to be removed. Again, this is done by integration by parts.

3. Third, also all derivatives on the smearing function are moved onto the remaining part of the integrand using integration by parts unless this results in a derivative on a delta-function. It should be noted that at this point boundary terms do appear and should be retained. (Important to observe that $g'(R^2) = \frac{\mathrm{d}g(R^2)}{\mathrm{d}R^2} = \frac{1}{2R}\frac{\mathrm{d}g(R^2)}{\mathrm{d}R}$.)

4. Fourth, the resulting integral is expanded to the desired order and the boundary terms of the integration by parts are handled. The boundary terms need to be evaluated at zero and infinity and can be divided into three categories. However, first note that all boundary terms when evaluated at infinity are zero due to the compact support of the smearing function. The three categories are

   - Terms higher order in R: R^n where $n > 0$
   - Constant terms: R^0
   - Terms singular in R: R^n where $n < 0$

   The first category gives zero when evaluated at the lower boundary. The second category also poses no problems and is just added to the final result, however the last category is more delicate. This part is integrated and subsequently subtracted from the bulk term which is needed for the Hadamard regularization. This regularization procedure was introduced by Hadamard in 1932 and is defined as

$$P.f. \int_0^\infty \mathrm{d}x f(x) = \lim_{\epsilon\to 0} \int_\epsilon^\infty \mathrm{d}x f(x) - P\left(\epsilon, \ln\epsilon\right),$$

   where $P.f.$ stands for *partie finie* (finite part) and P is a polynomial of the form

$$\sum_{n,m} a_{n,m}\epsilon^n \ln^m \epsilon,$$

   where $a_{n,m}$ are constants that generally depend on the value of $f(x)$ and its derivatives at $x = 0$ [18]. Let us consider an example to illustrate how the boundary terms produce exactly the terms that are needed to make the integral finite (so these boundary terms correspond to the polynomial $P(\epsilon, \ln\epsilon)$ in the above equation). We take two derivatives on the smearing function and a logarithm, then by continuity we have

$$\begin{aligned}\int_0^\infty \mathrm{d}x\, g''(x)\ln x &= \lim_{\epsilon\to 0}\int_\epsilon^\infty \mathrm{d}x\, g''(x)\ln x \\ &= \lim_{\epsilon\to 0}\left(\left[g'(x)\ln x\right]_\epsilon - \left[g(x)\frac{1}{x}\right]_\epsilon - \int_\epsilon^\infty \mathrm{d}x\, g(x)\frac{1}{x^2}\right) \\ &= P.f.\int_0^\infty \mathrm{d}x\,\frac{1}{x^2}g(x),\end{aligned}$$

   where in the second line we integrate by parts twice. The *partie finie* is thus defined in terms of these boundary terms. The boundary terms in the second line need to be evaluated at ϵ, however, they can also be integrated and taken under the integral sign so that all terms are on equal footing. We will use this principle too: all boundary terms that are singular in R are integrated first and then subtracted from the bulk terms to obtain the *partie finie*. This procedure provides us with a check on step two and three where all integrations by parts are performed: all singular boundary terms will need to be canceled by the bulk part.

5. Lastly, the integration over R is carried out according to the following rule

$$\int_0^\infty \mathrm{d}R\, g(R^2)\, R^n (\ln R)^m = \mu_{(n,m)}^{n-2} (\ln|\bar{\mu}_{(n,m)}|)^m, \tag{5.19}$$

where the different $\mu_{(n,m)}$ and $\bar{\mu}_{(n,m)}$ are distinct moments of the smearing function. For simplicity, we take all $\bar{\mu}_{(n,m)} = \mu_{(n,m)} = \mu$.

These steps will be summarized in the following master equation. However, we first introduce the following notation. Observing the tensorial coefficient in the expression for r in eq. (3.11), we see that we can write this coefficient as

$$r_{nX}^{Kij} = X^i A_{nX}^{Kj}$$

where X^i is a vector together with the numerical coefficient in front of each term appearing in eq. (3.11) and A_{nX}^{Kj} is the tangent vector to the line line segment X plus information on the number of derivatives acting on the gravitational field (K) and the number of iterated integrals (n). This gives for $\langle \tilde{r}^2 \rangle$

$$\begin{aligned}
\langle \tilde{r}^2 \rangle &= \frac{\ell_p^2}{2\pi} \sum_{KnX} \sum_{LmY} (-1)^{|L|}\, r_{nX}^{Kij}\, \eta_{ij,kl}\, r_{mY}^{Lkl} \sum_T T_{K\cup L} \sum_{d,\gamma,p} C_{d,\gamma,p}^{m,n} \\
&= \frac{\ell_p^2}{2\pi} \sum_{KnX} \sum_{LmY} (-1)^{|L|}\, X^i Y^k A_{nX}^{Kj} B_{mY}^{Ll} \eta_{ij,kl} \sum_T T_{K\cup L} \sum_{d,\gamma,p} C_{d,\gamma,p}^{m,n} \\
&= \frac{\ell_p^2}{2\pi} \sum_{n,m} \sum_{X,Y} \sum_T \sum_{K\cup L} (-1)^{|L|}\, X^i Y^k A_{nX}^{Kj} B_{mY}^{Ll} \eta_{ij,kl} T_{K\cup L} \mathcal{C}_{XY}^{m,n}[[T]] \\
&= \frac{\ell_p^2}{2\pi} \sum_{n,m} \sum_{X,Y} \Bigg(\sum_{T_0} \eta_{ij,kl} X^i Y^k A_{nX}^j\, T_0\, B_{mY}^l \mathcal{C}_{XY}^{m,n}[[T_0]] + (-1)^{|L|} \sum_{T_1} \sum_a \eta_{ij,kl} X^i Y^k A_{nX}^{aj}\, (T_1)_a\, B_{mY}^l \mathcal{C}_{XY}^{m,n}[[T_1]] \\
&\quad - \sum_{T_2} \sum_{a,b} \eta_{ij,kl} X^i Y^k A_{nX}^{aj}\, (T_2)_{ab}\, B_{mY}^{bl} \mathcal{C}_{XY}^{m,n}[[T_2]] \Bigg) \\
&= \frac{\ell_p^2}{2\pi} \sum_{n,m} \sum_{X,Y} \eta_{ij,kl} X^i Y^k \Bigg(\sum_{T_0} A_{nX}^j T_0 B_{mY}^l \mathcal{C}_{XY}^{m,n}[[T_0]] + (-1)^{|L|} \sum_{T_1} \sum_a A_{nX}^{aj} (T_1)_a B_{mY}^l \mathcal{C}_{XY}^{m,n}[[T_1]] \\
&\quad - \sum_{T_2} \sum_{a,b} A_{nX}^{aj} (T_2)_{ab} B_{mY}^{bl} \mathcal{C}_{XY}^{m,n}[[T_2]] \Bigg) \\
&= \frac{\ell_p^2}{2\pi} \sum_{n,m} \sum_{X,Y} \eta_{ij,kl} X^i Y^k E^{jl},
\end{aligned}$$

where E^{jl} is defined implicitly by the last two lines. The coefficient $C_{d,\gamma,p}^{m,n}$ corresponds to the result that is stored in the tables (i.e. the integrated result after 'part I'), and $\mathcal{C}_{XY}^{m,n}[[T_k]]$ is the result after both 'part I' and 'part II' have been performed, where the double square brackets denote the dependence on the tensor basis element. Going from the third to the fourth equality, the factor $(-1)^{|L|}$ gives a plus sign for the terms that correspond to all tensor basis elements T_0 and a minus sign for T_2. For the tensor basis elements T_1, it contributes a plus or minus sign depending on whether A_{nX}^{Kj} or B_{mY}^{Ll} carries the derivative on the smearing function. The routine for each term in $\langle \tilde{r}^2 \rangle$ is illustrated in the flow-chart in fig. 5.4. This process is repeated for each term after which the sum over all terms is performed (i.e. the sum over n, m and X, Y in the equation above) to obtain $\langle \tilde{r}^2 \rangle$.

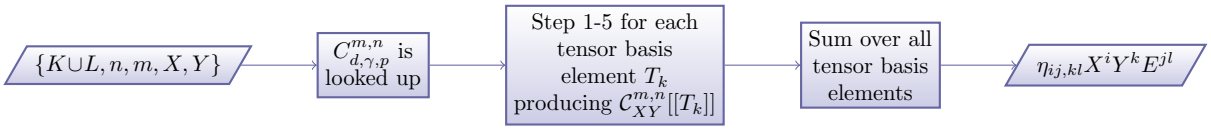

Figure 5.4: Flow-chart summarizing the process that the computer routine performs for each term in $\langle \tilde{r}^2 \rangle$. Step 1-5 refer to the steps outlined in this section. Notation regarding the symbols is explained in the text. Once all terms are computed, these are added to yield $\langle \tilde{r}^2 \rangle$.

Chapter 6

Results

In this chapter, we will present the result for the variance of quantum fluctuations in observations of the emission time (from which one can easily obtain the variance of the time delay). As a sanity check on our result, we first perform a dimensional analysis closely following sec. VII,D in [3]. In the second part, the result is presented in various forms. The chapter ends with a presentation of all checks on the result.

6.1 Dimensional analysis

The term that contributes most to the final answer is the most divergent term. As divergences are worsened by derivatives and softened by integrals, the most divergent term should have the maximal number of derivatives and minimal number of integrals. Looking at eq. (5.3), we find that this corresponds to two derivatives on $\{h_X, h_Y\}$ and two single integrals along the line segments, i.e. $r^2 \sim r^X r^Y \int_X \int_Y \nabla^2 h_X h_Y$. The derivative operator ∇ has length dimension -1, the gravitational field and r are both dimensionless and since we have parametrized our line integrals to run from zero to one $\int_X$ is also dimensionless. Therefore, the tensorial coefficient r^X needs to have length dimension $+1$ and be of order s, where s is the length scale of the corresponding line segment. The expectation value of the anti-commutator of the gravitational field is proportional to ℓ_p^2/z^2, where z is a spacetime interval, thus $[\ell_p] = [z] = 1$. The only length scale left is the detector resolution μ which also has length dimension $+1$. Thus, the most divergent term in $\langle \tilde{r}^2 \rangle$ should be of the form

$$\begin{aligned}
\langle \tilde{r}^2 \rangle &\sim \langle r^X r^Y \int_X \int_Y \nabla^2 \{h_X, h_Y\} \rangle \\
&\sim s^2 \langle \int_X \int_Y \nabla^2 \frac{\ell_p^2}{z^2} \rangle \\
&\sim s^2 \langle \int_X \int_Y \frac{\ell_p^2}{z^4} \rangle \\
&\sim s^2 \langle \frac{\ell_p^2}{s^2 z^2} \rangle \sim \frac{\ell_p^2}{\mu^2}
\end{aligned}$$

where we used that $\int_X z^n \sim z^{n+1}/s$ and in this particular case $\langle \ldots \rangle$ denotes smearing as well as taking the expectation value. Thus, from this simple dimensional argument we do not expect terms that are more divergent than $1/\mu^2$. Clear from this expression is that when $\mu \to 0$ $\langle \tilde{r}^2 \rangle$ diverges, as it should because this limit corresponds to not doing any smearing and we already knew that the unsmeared result should be infinite. Thus, for sharper detector resolution effects due to quantum fluctuations grow. Such quantum fluctuations are vividly illustrated in the context of quantum optics in fig. 2.1 of [19].

6.2 First order quantum corrections to the time delay observable

The experimental input is completely determined by the length scale set by the reception time s and the relative speed between the worldlines of the lab and the probe which is related to the (positive) hyperbolic rapidity by $v_{rel}/c = \tanh(\theta)$. Given these two numbers s and v_{rel}, the mean and the variance of the quantum fluctuations in the emission time can be exactly obtained to linear order in the gravitational field from the computer routine. Let us recall the expansion in the gravitational field for the emission time as defined in ch. 3

$$\tilde{\tau}(s) = e^{\tilde{r}(\tilde{h})}\tau_{cl}(s) = \tau_{cl}(s)(1 + r(\tilde{h}) + \mathcal{O}(h^2)).$$

From this expression, we defined in ch. 4 the quantum mean and the variance of the emission time by

$$\mu_\tau = \langle\tilde{\tau}(s)\rangle = \tau_{cl}(s) + \mathcal{O}(h^2) = se^{-\theta} + \mathcal{O}(h^2),$$
$$\sigma_\tau^2 \sim \tau_{cl}^2(s)\,\langle\tilde{r}^2\rangle + \mathcal{O}(h^2) = s^2e^{-2\theta}\,\langle\tilde{r}^2\rangle + \mathcal{O}(h^2).$$

The quantum mean

The quantum mean of the emission time is to linear order the same as τ_{cl}, which is

$$\mu_\tau = se^{-\theta} = se^{-\text{arctanh}(v_{rel}/c)} = s\sqrt{\frac{1 - \frac{v_{rel}}{c}}{1 + \frac{v_{rel}}{c}}}. \tag{6.1}$$

In fig. 6.1, the mean of the quantum fluctuations in the emission time is shown for all physically allowed relative velocities.

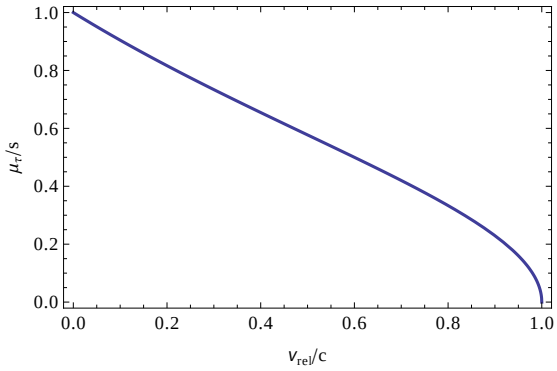

Figure 6.1: Plot of $\mu_\tau/s = e^{-arctanh(v_{rel}/c)}$ versus v_{rel}/c to linear order in the gravitational field.

The quantum variance

The quantum variance of the emission time to linear order in the gravitational field is given by $\sigma_\tau^2 = \langle\tau^2\rangle - \langle\tau\rangle^2 \sim s^2e^{-2\text{arctanh}(v_{rel}/c)}\langle\tilde{r}^2\rangle$. The expectation value of $\tilde{r}^2$ is shown to be of the form

$$\langle\tilde{r}^2\rangle = \frac{\ell_p^2}{\mu^2}\left(\rho_0 + \rho_1\frac{\mu}{s} + \rho_2\frac{\mu^2}{s^2} + \mathcal{O}\left(\frac{\mu}{s}\right)^3\right) + \mathcal{O}\left(\frac{\ell_p}{\mu}\right)^2, \tag{6.2}$$

where the coefficients ρ_i's are in general functions of v_{rel}/c and the overall factor $\frac{1}{2\pi}$ in eq. (5.1) is canceled by the 2π from the angular integration. Also note that the result is given to order

$\mathcal{O}(\ell_p/\mu)^2$ as we did not include $\tilde{r}_2(h)$ in our calculation for the variance. Albeit terms proportional to $\ln\mu$ appear in intermediate results, they are remarkably all canceled in the final expression for $\langle\tilde{r}^2\rangle$.

In tab. 6.2, numerical values for the root-mean square size of the quantum fluctuations in observations of the emission time (σ_τ) are presented for two different experimental settings: a laboratory one, which is set by a length scale $s \sim 1\,\mathrm{m} \sim 10^{-9}$ s and a cosmological one, which has $s \sim 1\,\mathrm{Mpc} \sim 10^{22}\,\mathrm{m} \sim 10^{14}\,\mathrm{s}$. The spatio-temporal resolution of the detector is taken to be of the order of X-rays, i.e., $\mu \sim 1\,\mathrm{nm} \sim 10^{-18}\,\mathrm{s}$, which is realistic for both settings. The leading order contribution to σ_τ is determined by the Planck length ($\ell_p \sim 10^{-35}\,\mathrm{m} \sim 10^{-44}\,\mathrm{s}$) divided by the detector resolution and is of the order $\ell_p/\mu \sim 10^{-27}$. The table shows numerical values for four relative velocities: 1 m/s, the recession time of a distant galaxy ($\sim 10^5$ m/s for a galaxy at 1 Mpc), $c/2$ and $99c/100$. The values presented for the cosmological scale should be read critically as the validity of the linearized approximation to regimes for large s/μ ratios is still under investigation. This concern was already raised in [3]. Note that apart from values corresponding to large s and small v_{rel}/c, which we should be skeptical about, all other values for the root-mean-square size of the quantum fluctuations are well below the sensitivity or noise thresholds of the current state of experimental and observational technology. Hence, it is not surprising that this kind of effect has not yet been observed. Furthermore, there are eight orders of magnitude difference between the values corresponding to $v_{rel} = 1$ m/s and $v_{rel} = 99c/100$. At the moment, we do not know of an explanation for this huge increase in the root-mean-square size of the quantum fluctuations. The output for $\langle\tilde{r}^2\rangle$ in terms of symbolic expressions for v_{rel}/c may shed light on this behavior. Although, it could be possible that the $\tilde{r}_2(h)$ term may contribute significantly at this order and change this behavior completely.

v_{rel}	1 m/s	10^5 m/s	$\frac{c}{2}$	$\frac{99c}{100}$
$s = 1$ m	10^{-18}	10^{-23}	10^{-26}	10^{-26}
$s = 1$ Mpc	10^4	10^{-1}	10^{-4}	10^{-4}

Table 6.1: The root-mean-square size of quantum fluctuations in observations of the emission time σ_τ in seconds for a detector sensitivity $\mu = 1$ nm for two different contexts: a laboratory setting ($s = 1$ m) and a cosmological setting ($s = 1$ Mpc).

v_{rel}	$\langle\tilde{r}^2\rangle/(\ell_p/\mu)^2$
$\frac{c}{10}$	$\frac{5881}{8} - 3366\ln\left(\frac{11}{9}\right) - 2\pi^2\frac{\mu}{s}$
$\frac{2c}{10}$	$217 - 456\ln\left(\frac{3}{2}\right) - 2\pi^2\frac{\mu}{s}$
$\frac{3c}{10}$	$\frac{921}{8} - \frac{1274}{9}\ln\left(\frac{13}{7}\right) - 2\pi^2\frac{\mu}{s}$
$\frac{4c}{10}$	$\frac{2479}{32} - \frac{483}{8}\ln\left(\frac{7}{3}\right) - 2\pi^2\frac{\mu}{s}$
$\frac{5c}{10}$	$\frac{473}{8} - 30\ln(3) - 2\pi^2\frac{\mu}{s}$
$\frac{6c}{10}$	$\frac{146}{3} - 32\ln(2) - 2\pi^2\frac{\mu}{s}$
$\frac{7c}{10}$	$\frac{16489}{392} - \frac{2958}{343}\ln\left(\frac{17}{3}\right) - 2\pi^2\frac{\mu}{s}$
$\frac{8c}{10}$	$\frac{4811}{128} - \frac{279\ln(3)}{32} - 2\pi^2\frac{\mu}{s}$
$\frac{9c}{10}$	$\frac{7427}{216} - \frac{418\ln(19)}{243} - 2\pi^2\frac{\mu}{s}$
c	$\frac{1}{e^{-2\mathrm{arctanh}(1)}}(29 - \frac{\pi^2}{4}\frac{\mu}{s})$

Table 6.2: This table shows $\langle\tilde{r}^2\rangle/(\ell_p/\mu)^2$ for various v_{rel} to linear order in the gravitational field. The dependence on the reception time s is made explicit.

As noted before, the coefficients ρ_i in eq. (6.2) are in general functions of v_{rel}/c, however, we do not have these functions explicitly at the moment, since the computer code computes these coefficients separately for each input. It should not be too difficult to massage the computer routine to output symbolic expressions for the ρ_i's, however, this is left for future research.[1] The expressions for $\langle\tilde{r}^2\rangle/(\ell_p/\mu)^2$ are shown for various relative velocities between zero and the speed of light in tab. 6.2. Note that $\langle\tilde{r}^2\rangle$ is dimensionless (and hence also all entries in this table are). Furthermore, observe that the coefficient ρ_1 is $-2\pi^2$ for all relative velocities (except for $v_{rel} = c$, which will be discussed shortly) and all ρ_2 coefficients equal zero, consequently, ρ_1 and ρ_2 are independent of v_{rel}/c and all dependence on the relative velocity is captured by ρ_0. This behavior was not obvious a priori and one of the motivations for this computation. Additionally, it should be noted that the factor multiplying the result for $v_{rel} = c$ ($\frac{1}{e^{-2\mathrm{arctanh}(1)}}$) is divergent, however, when calculating σ_τ^2 this factor is canceled as it is again multiplied by $e^{-2arctanh(1)}$.

A plot of the coefficient ρ_0 versus v_{rel}/c is shown in fig. 6.2. As is clear from the graph ρ_0 diverges for the limit $v_{rel}/c \to 0$ after which it decreases for increasing v_{rel}/c and reaches a minimum, after this minimum it increases again. In the limit $v_{rel}/c \to 1$ it seems as if the graph is discontinuous. The lack of continuity could be explained by the fact that one of the line segments along which we integrate changes from being timelike to null and this may result in terms with very different singularity structures for the smeared integrals that enter into the evaluation of $\langle\tilde{r}^2\rangle$. Since we have no reason to expect discontinuous dependence on v_{rel}/c, such an apparent discontinuity should be resolved into a smooth transition on an interval of the size v_{rel}/c in $[1-\mu/s, 1]$ if we would compute the result exactly. Unfortunately, our approximation methods (effectively we expand in powers of μ/s) do not allow us to resolve this smooth transition. A similar argument can be made for the limit in which $v_{rel}/c \to 0$. Therefore, the results in the transition regions $[0, \mu/s]$ and $[1-\mu/s, 1]$ are not reliable at present. (The numerical values presented in tab. 6.1 fall outside these regions as typically $\mu/s \leq 10^{-9}$ and are thus not affected by this point.) In addition, the minimum of ρ_0 selects a preferred velocity between 0 and c, which is at odds with Lorentz invariance. This is not surprising, since our choice for the smearing function explicitly broke Lorentz invariance. It would be interesting to see the behavior of ρ_0 as a function of v_{rel}/c for a Lorentz invariant smearing function. This may be addressed by future research.

The coefficient ρ_0 in $\langle\tilde{r}^2\rangle$ has exactly the same form as predicted by the dimensional analysis in the previous section. The coefficient ρ_1, which precedes the subleading terms in μ/s, is negative for all relative velocities, which indicates that larger ratios of μ/s (corresponding to a less sensitive detector given the same reception time) tend to suppress the quantum fluctuations. This relation is shown in fig. 6.3, which is a log-log plot of σ_τ/ℓ_p versus μ/s for various v_{rel}/c. It is also clear from this graph that the dominant contribution to the variance changes only for $\mu/s > 1$.

The calculation time can be divided into two parts, similar to 'part I' and 'part II' in ch. 5: generating the tables (which only needs to be done once) and the explicit calculation of $\langle\tilde{r}^2\rangle$. On a standard computer (AMD 64 Dual Core 2 GHz Processor) the first part takes approximately 45 minutes and the second part takes about 20 minutes. The most time consuming part in this latter calculation is the expansion in $b \cdot \hat{u}$ for non-parallel line segments. If this expansion could also have been tabulated, the calculation time for $\langle\tilde{r}^2\rangle$ would be drastically reduced. For more details on this expansion, see sec. 5.2 in ch. 5.

6.3 Checks on result

In this section, we will discuss several checks that we implemented to make sure that we can be confident that the result presented is correct. First of all, as discussed in ch. 2, all physical

[1] In fact, the computer routine also does not show the explicit dependence on the reception time s, however, the dependence on s can easily be obtained by comparison of the expressions generated by the computer for various s while keeping the relative velocity constant and by dimensional arguments.

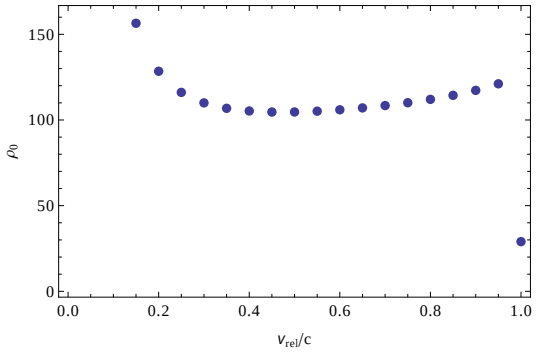

Figure 6.2: Plot of ρ_0 versus v_{rel}/c. This curve is the same for all values of s. Note the discontinuity in the plot for $v_{rel}/c = 1$.

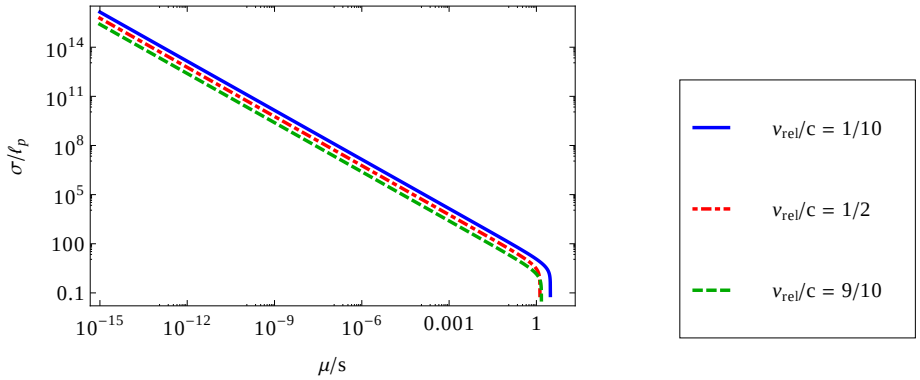

Figure 6.3: A log-log plot of σ_τ/ℓ_p versus μ/s for various v_{rel}/c. The length scale s is set to $1m$.

observables need to satisfy the positivity requirement. It is obvious from the graph in fig. 6.2 that $\langle \tilde{r}^2 \rangle$ is, fortunately, always positive and this serves as a first check on our result. In addition, as was remarked in ch. 3, parts of the expression of r, H and J, are independently invariant under linearized diffeomorphism. These parts turn out to satisfy all other constraints on observables as well and are thus strictly speaking also observables, although their physical interpretation is not directly clear. Thus, H^2 and J^2 and any positive functional thereof should also be equal to or larger than zero. This was checked by the same routine that was used to calculate $\langle \tilde{r}^2 \rangle$ and indeed it was shown that $H^2 \geq 0$ and $J^2 \geq 0$.

Second, the results nicely match the predictions made by the simple dimensional analysis: no terms more divergent than $1/\mu^2$ appear. In [3], it was noted that detailed calculations reveal terms with a more divergent scaling behavior (these terms are of the form $\ell_p^2/\mu^2 \ln \mu/s$ and $s\ell_p^2/\mu^3$), however, these terms cancel in the final result.

Third, there are two independent parts in our calculation where we expected intermediate results in the integrals to cancel each other in the final summations over all endpoints of the parallelogram. One of these expected cancellations was already mentioned in ch. 5: for the case $b \cdot \hat{u} = 0$, we expanded the result in $b \cdot \hat{u}$ and only retained the zeroth order term, the lower order terms were not considered. An independent routine checked whether we rightfully had thrown away the lower order terms: the outcome was positive, all lower order terms vanish in the final summations over the overall $\pm$-sign, $c = \pm R$ and the four vertices. The other part where we expected calculations to happen was related to the integration over c. This integration may produce terms that have the 'wrong' powers of R, which would eventually lead to terms scaling as $1/\mu^4$. Fortunately, these terms vanish when the boundaries of the c-summation are taken into

account (so the summation over the $\pm$-sign and $c = \pm R$ is performed).

Fourth, as a check on the internal consistency of the routine that handles all integration by parts, the boundary terms produced by removing all derivatives from the smearing function nicely cancel with divergent terms in the bulk. This check is discussed in detail at the end of ch. 5.

Lastly, the integral $\tilde{I}_K^{mn}(X;Y)$ has been calculated by hand for a simple case: $m = n = 0$ (hence no iterated integrals) and along two parallel null-like line segments. This has been done for zero, one as well as two derivatives on the smearing function, that is, $K = 0, 1, 2$. The results of the calculation by hand match exactly the result produced by the computer routine and can be found in app. C.

All in all, these partial checks of various aspects of the calculation make us confident that the result presented is correct.

Chapter 7

Discussion

In this chapter, a summary of what has been done will be given. Next, recommendations for future research are discussed.

7.1 Summary

As mentioned before, this work is a follow-up on [3]. In that work, a physical observable in the context of quantum gravity was defined by means of a clock synchronization thought experiment. In this thesis, we recapped the set-up of this thought experiment after which we have presented the explicit calculation, to linear order in the gravitational field, for the variance of the quantum fluctuations in the emission time. For this calculation, we resorted to the use of computer algebra software due to the large amount of integrals that needed to be evaluated.

The results show that the quantum mean of the emission time is given by $se^{-\operatorname{arctanh}(v_{rel}/c)}$, where s is the reception time and v_{rel} is the relative velocity between the worldlines of the lab and the probe. The results for the quantum variance of the emission time are all of the form

$$\sigma_\tau^2 = 4s^2 \exp\left(-2\operatorname{arctanh}(v_{rel}/c)\right) \frac{\ell_p^2}{\mu^2} \left(\rho_0 + \rho_1 \frac{\mu}{s} + \mathcal{O}\left(\frac{\mu}{s}\right)^3\right) + \mathcal{O}\left(\left(\frac{\ell_p}{\mu}\right)^2\right),$$

where ρ_0 depends on v_{rel}/c and $\rho_1 = -2\pi$ for all physically allowed v_{rel}/c. The behavior of the coefficient ρ_0 is rather surprising: it is very large in the limit $v_{rel}/c \to 0$, then decreases for increasing v_{rel}/c until it hits a minimum after which it slowly increases again. This minimum selects a preferred v_{rel}/c, which breaks Lorentz invariance. This may be due to the fact that our choice of smearing also broke Lorentz invariance, however, this is speculative and requires further research. It should be noted that even though ρ_0 shows a non-trivial behavior depending on v_{rel}/c, the total quantum variance only shows a decreasing trend for increasing v_{rel}/c. Furthermore, given the reception time s, the quantum variance of the emission time increases when a more sensitive detector is used. Thus, a less sensitive detector suppresses the quantum fluctuations of the gravitational field. This effect also occurs in quantum optics and is not surprising.

The size of the quantum fluctuations is for most values below current experimental and observational sensitivity or noise thresholds except for experimental settings corresponding to cosmological scales and a very small relative velocity between the lab and probe worldline. These values are possibly not valid due to the limitations of the linear order approximation to the geodesic equations. Assuming for now that these approximations hold for cosmological scales with large relative velocities, the quantum fluctuations for the variance of the emission time are several orders of magnitude below the current detector sensitivity and, thus, with increasing understanding of observational data the noise threshold may be reduced to a level at which

this effect may be observed. Clearly, this calculation should be adapted to fit the set-up of the relevant observations and the validity of the linearized approximation to regimes for large s/μ should be reassessed.

Two motivations for this calculation were to see whether we can construct physical observables operationally and to probe the causal structure of spacetime. From this discussion, it is clear that by 'working backwards', i.e., using an experimental protocol, a whole class of physical observables with manageable calculations can indeed be defined. As was suggested in [3], we will refer to this class of observables as *(quantum) astrometric observables*. Unfortunately, due to the broken Lorentzian signature, we were not able to study the causal structure of spacetime non-perturbatively.

7.2 Recommendations

Several simplifications were made to make the calculation feasible at this stage. One of them was already mentioned in ch. 4: we ignored the $r_2(\hat{h})$ term in our calculation for the variance of the emission time, while in fact we should have included this term to have a correct expansion to linear order in the gravitational field. Future research may address this point. Another simplification that was also already mentioned in the same chapter was our choice for the smearing function. The choice we made breaks background Lorentz invariance, which is unphysical. A more physical smearing function should be chosen. This should also address the behavior of the coefficient ρ_0 in eq. (6.2) which for our choice of smearing seems to select a preferred relative velocity. In addition, it may be interesting to see how other choices of smearing affect the final result. Although it is expected that a kind of universality among all well-behaved localized smearing functions exists for the leading divergent terms and thus should not affect the final answer too much.

In addition, the calculation carried out in this thesis was specific for the triangular experimental set-up. However, the calculation is flexible to an arbitrary polygon restricted to a plane that consists of time-like and null-like edges. This is because the bulk of the work is concerned with the evaluation of the integrals $\tilde{I}_K^{mn}$. The computer algebra software is able to handle any such integral, thus, the quantum mean and variance of a 'time delay' observable or any other related observable in an arbitrary 2-dimensional set-up can be straightforwardly computed. One only needs to calculate the mean and the equivalent expression for $\langle \tilde{r}^2 \rangle$ using the closure condition for the experimental set-up.

Furthermore, the expansion was done to zeroth order in the spatio-temporal resolution of the smearing function μ. This could be extended to higher order. However, this should not be of high priority as higher orders do not contribute much.

Additionally, we were not able to study the causal structure of spacetime in a quantum context as the perturbation technique used breaks the Lorentzian signature. As suggested before, this issue may be resolved using other perturbation techniques such as the Magnus expansion [8]. Another solution to this issue could be to resort to situations for which non-perturbative calculations are possible such as 2+1 gravity.

More generally, we can now model other observables within the field of quantum gravity by using a similar methodology. Observables that may be of particular interest are those related to black holes or the early universe as quantum gravitational effects are expected to be largest in those regimes. For instance, one may want to model the fluctuations of area of the black hole horizon. This would allow one to study the fluctuations of the size of a black hole, since the radius of a black hole is defined via its area.

Moreover, in this work, we used Minkowski spacetime as our background, but other metric such as the Schwarzschild metric or FRW-metric could be considered. This may be interesting for actual experiments. A hot research area that possibly allows us to probe the quantum nature of the gravitational field is research concerned with the observation of photons arriving from distant γ-ray bursts. A similar calculation as ours could model the arrival of these photons and

compute the quantum effects due to the intrinsic quantum nature of the gravitational field. [20]

Finally, it is often the case that calculations that are simple in one fundamental approach to quantum gravity are unfeasible in another, which makes comparing different fundamental approaches difficult. The future may tell whether this observable, or any other quantum astrometric observable, will be a useful benchmark for these fundamental approaches to quantum gravity.

Appendix A

Perturbative solution of geodesic and parallel transport equations

In this appendix, we derive the perturbative solution of the geodesic and parallel transport equations given the lab-equipped spacetime as discussed in ch. 3.3. The set-up of this derivation will be very similar to the appendix in [3], however, we display more intermediate steps.

For this derivation we need the following two equations [5]

$$\dot{\gamma}(t)^a = v_0^a(t), \tag{A.1}$$
$$\dot{\gamma}(t)^a \nabla_a v_\alpha^c(t) = 0, \tag{A.2}$$

where the first equation states that v_0^a is the tangent vector to the geodesic $\gamma(t)$ and the second equation is the geodesic equation, i.e. it describes a curve whose tangent vector v^c is parallel propagated along itself. These equations (A.1,A.2) can be expressed in terms of vierbein components using the relations in chapter 3.3. The first equation gives

$$\begin{aligned}\dot{\gamma}^i &= \dot{\gamma}^a \hat{x}_a^i = v_0^a \hat{x}_a^i \\ &= v_0^a \bar{T}_j^i e_a^j = \bar{T}_j^i v_0^j,\end{aligned} \tag{A.3}$$

where we used that $\hat{x}_a^i = \bar{T}_j^i e_a^j$. The second equation is first rewritten as

$$\begin{aligned}\dot{\gamma}^a \nabla_a v_\alpha^c &= 0 \\ v_0^a \nabla_a (e_j^c v_\alpha^j) &= 0 \\ v_0^a e_j^c \nabla_a (v_\alpha^j) &= -v_0^a \nabla_a (e_j^c) v_\alpha^j,\end{aligned}$$

to obtain in vielbein components

$$\begin{aligned}v_0^a \nabla_a (v_\alpha^k) &= -v_0^i e_i^a e_c^k \nabla_a (e_j^c) v_\alpha^j, \\ \dot{v}_\alpha^k &= -v_0^i \omega_i{}^k{}_j v_\alpha^j,\end{aligned} \tag{A.4}$$

where $\omega_i{}^k{}_j$ are the Ricci rotation coefficients (see sec. 3.4b in [5]). These Ricci rotation coefficients can be expressed in terms of the transformation matrix $T^i{}_j$, which will be done below so that we can express the Ricci rotation coefficients in terms of the gravitational field. Below, $\partial_a = \hat{x}_a^i \partial_i$ denotes the coordinate derivative, ∇_a the covariant derivative and Γ_{ab}^c the usual Christoffel tensor

$$\begin{aligned}\omega_{ikj} &= e_{kc} e_i^a \nabla_a e_j^c \\ &= e_{kc} e_i^a \partial_a e_j^c + e_{kc} e_i^a \Gamma_{ab}^c e_j^b \\ &= e_{kc} e_i^a \partial_a e_j^c + e_i^a e_j^b e_k^c \Gamma_{cab}.\end{aligned}$$

The first term in the equation can be rewritten using eq. (3.1) and gives

$$\begin{aligned} e_{kc}e_i^a\partial_a e_j^c &= \bar{T}_i^{i'}(\partial_a \bar{T}_j^{j'})T_{l'}^l \eta_{lk}\hat{x}_c^{l'}\hat{x}_{i'}^a\hat{x}_{j'}^c \\ &= \bar{T}_i^{i'}(\partial_{i'}\bar{T}_j^{l'})T_{l'}^l\eta_{lk} \\ &= -\bar{T}_i^{i'}\bar{T}_j^{j'}(\partial_{i'}T_{j'}^{l''})\bar{T}_{l''}^{l'}T_{l'}^l\eta_{lk} \\ &= -\bar{T}_i^{i'}(\partial_{i'}T_{j'}^l\eta_{lk})\bar{T}_j^{j'}, \end{aligned}$$

and similarly for the second term

$$\begin{aligned} e_i^a e_j^b e_k^c \Gamma_{cab} &= \frac{1}{2}e_i^a e_j^b e_k^c(\partial_a g_{bc} + \partial_b g_{ac} - \partial_c g_{ab}) \\ &= \frac{1}{2}\bar{T}_i^{i'}\bar{T}_j^{j'}\bar{T}_k^{k'} \\ &\quad \times [\partial_{i'}g_{j'k'} + \partial_{j'}g_{i'k'} - \partial_{k'}g_{i'j'}] \\ &= \frac{1}{2}\bar{T}_i^{i'}\bar{T}_j^{j'}\bar{T}_k^{k'}\left[\partial_{i'}(T_{j'}^J\eta_{JK}T_{k'}^K)\right. \\ &\quad \left. + \partial_{j'}(T_{i'}^I\eta_{IK}T_{k'}^K) - \partial_{k'}(T_{i'}^I\eta_{IJ}T_{j'}^J)\right]. \end{aligned}$$

Substituting the following definition $\alpha_{ikj} = \bar{T}_i^{i'}(\partial_{i'}T_{j'}^l\eta_{lk})\bar{T}_j^{j'}$ in both equations and adding them again yields the following expression for the Ricci rotation coefficients in terms of this single quantity α_{ikj}

$$\begin{aligned} \omega_{ikj} &= -\alpha_{ikj} + \frac{1}{2}\left[\alpha_{ikj} + \alpha_{ijk} + \alpha_{jik}\right. \\ &\quad \left. + \alpha_{jki} - \alpha_{kij} - \alpha_{kji}\right] \\ &= \frac{1}{2}\left[-\alpha_{ikj} + \alpha_{ijk} + \alpha_{jik}\right. \\ &\quad \left. + \alpha_{jki} - \alpha_{kij} - \alpha_{kji}\right] \\ &= -3\alpha_{[ikj]} + 2\alpha_{[j|i|k]} \\ &= -\alpha_{i[kj]} + \alpha_{j(ik)} - \alpha_{k(ij)}. \end{aligned}$$

According to standard conventions, square brackets around tensor indices indicate that the tensor is anti-symmetric with respect to these indices and round brackets indicate that the tensor is symmetric. Up to linear order in the gravitational field, α_{ikj} is given by

$$\begin{aligned} \alpha_{ikj} &= \bar{T}_i^{i'}(\partial_{i'}T_{j'}^l\eta_{lk})\bar{T}_j^{j'} \\ &= (\delta_i^{i'} - h_i^{i'})(\partial_{i'}h_{j'}^l\eta_{lk})(\delta_j^{j'} - h_j^{j'}) \\ &= \partial_i h_j^l\eta_{lk} + \mathcal{O}(h^2) = \partial_i h_{kj} + \mathcal{O}(h^2), \end{aligned}$$

where we used that $T = \exp(h)$ and $\bar{T} = \exp(-h)$. Consequently, up to linear order the Ricci rotation coefficient is given by

$$\omega_{ikj} = -\partial_i h_{[kj]} + \partial_j h_{(ik)} - \partial_k h_{(ij)}.$$

Looking back at eq.(A.3) and eq.(A.4), we are left with two differential equations. These two differential equations are of the form

$$\dot{X}(t) = \lambda\, A(t)\, X(t),$$

where $|\lambda| \ll 1$ and $X(t)$ can be any $n-$column vector and $A(t)$ any $n \times n-$matrix. In the simple case where $A(t)$ is a constant, i.e. $A(t) = A_0$, the solution to this differential equation is

$X(t) = e^{\lambda A_0 t} X(0) = X_0(t) + \lambda X_1(t) + \lambda^2 X_2(t) + \mathcal{O}(\lambda^3)$. However, if $A(t)$ is not constant, then the solution is

$$\begin{aligned} X(t) &= X(0) + \lambda \int_0^t \mathrm{d}t' A(t') X(0) + \lambda^2 \int_0^t \mathrm{d}t' \int_0^{t'} \mathrm{d}t'' A(t') A(t'') X(0) + \mathcal{O}(\lambda^3) \\ &:= T\left[\exp\left(\lambda \int_0^t \mathrm{d}t' A(t')\right)\right] X(0), \end{aligned}$$

where T denotes the time ordered exponential. If $A = A(t, X(t))$ the above solution still holds, but now $A(t')$ should be replaced by $A(t', X(t'))$. The solutions to eq. (A.3) and eq. (A.4) are thus given by

$$\gamma(t)^i = \gamma(0)^i + \int_0^t \mathrm{d}t'\, \bar{T}(\gamma(t'))^i_j v_0^j(t'), \tag{A.5}$$

$$\begin{aligned} v_\alpha^k(t) &= T\left[\exp\left(-\int_0^t \mathrm{d}t' v_0(t')^i \omega(\gamma(t'))_i{}^k{}_j\right)\right] v_\alpha^j(0) && \text{(A.6)} \\ &= \exp(p_\gamma(t))^k_j v_\alpha^j(0), && \text{(A.7)} \end{aligned}$$

where the parallel propagator $\exp(p_\gamma(t))^k_j$ is defined implicitly by the last equation. In this form, the solution can be directly expanded to any desired order in the gravitational field h and are parametrized by the initial data $\gamma(0)^i$ and $v_\alpha^i(0)$ with $\dot{\gamma}^i(0) = v_0^i(0)$.

For our experimental set-up, some vectors will be parallel transported more than once. For example, consider a geodesic β starting at the origin $\beta(0) = O$ and a geodesic γ whose starting point is the end point of β (i.e. $\beta^i(1) = \gamma^i(0)$). If we want to parallel transport some vector at the origin, say $v_{O,\alpha}^k$, along β and γ, we have for the vierbein components of the parallel transported vector at the starting and end point of the geodesic γ

$$\begin{aligned} v_\alpha^i(0) &= \exp(p_\beta)^i_j \exp(h_O)^j_k v_{O,\alpha}^k, \\ v_\alpha^i(1) &= \exp(p_\gamma)^i_j \exp(p_\beta)^j_k \exp(h_O)^k_l v_{O,\alpha}^l. \end{aligned}$$

Further note that to linear order in the gravitational field, the parallel propagator is

$$\begin{aligned} \exp(p_\gamma(t))^k_j &= \delta^k_j + (H_{\gamma_0}(t))^k_j + \mathcal{O}(h^2), && \text{(A.8)} \\ (H_{\gamma_0}(t))_{kj} &= \eta_{ki}(H_{\gamma_0}(t))^i_j \\ &= -\int_0^t \mathrm{d}t'\, \dot{\gamma}_0^i(t') \omega(\gamma_0(t'))_{ikj}. && \text{(A.9)} \end{aligned}$$

Thus, to linear order the starting and end point of the parallel propagated vector is

$$\begin{aligned} v_\alpha^i(0) &= v_{O,\alpha}^i + (h_O)^i_j v_{O,\alpha}^j + (H_{\gamma_0})^i_j v_{O,\alpha}^j + \mathcal{O}(h^2) && \text{(A.10)} \\ v_\alpha^i(1) &= v_{O,\alpha}^i + (h_O)^i_j v_{O,\alpha}^j + (H_{\beta_0} + H_{\gamma_0})^i_j v_{O,\alpha}^j + \mathcal{O}(h^2). && \text{(A.11)} \end{aligned}$$

For the vielbein coordinates of the geodesic curve, the linear order solution is

$$\begin{aligned} \gamma^i(1) &= \beta^i(1) + \int_0^1 \mathrm{d}t'\, \exp(-h(\gamma(t')))^i_j \exp(p_\gamma(t'))^j_k \exp(p_\beta)^k_l \exp(h_O)^l_m v_{O,0}^m \\ &= \beta_0^i(1) + \beta_1^i(1) + \int_0^1 \mathrm{d}t'\, \left[-h^i_j(\gamma_0(t')) + (H_{\gamma_0}(t'))^i_j + (H_{\beta_0})^i_j + (h_O)^i_j\right] v_{O,0}^j + \mathcal{O}(h^2) \\ &= \beta_0^i(1) + \beta_1^i(1) - \int_0^1 \mathrm{d}t' h^i_j(\gamma_0(t')) v_{O,0}^j - \int_0^1 \mathrm{d}t' \int_0^{t'} \mathrm{d}t'' \dot{\gamma}_0^k(t'') \omega(\gamma_0(t''))_k{}^i{}_j v_{O,0}^j \\ &\quad + (H_{\beta_0})^i_j v_{O,0}^j + (h_O)^i_j v_{O,0}^j + \mathcal{O}(h^2) \\ &= \beta_0^i(1) + \beta_1^i(1) + (J_{\gamma_0,\beta_0})^i + \mathcal{O}(h^2), \end{aligned} \tag{A.12}$$

where $(J_{\gamma_0,\beta_0})^i$ is to linear order

$$\begin{aligned}(J_{\gamma_0,\beta_0})^i &= \eta^{ij}(J_{\gamma_0,\beta_0})_j \\ &= -\int_0^1 \mathrm{d}t' h^i_j(\gamma_0(t'))v^j_{O,0} - \int_0^1 \mathrm{d}t' \int_0^{t'} \mathrm{d}t'' \dot{\gamma}^k_0(t'')\omega(\gamma_0(t''))_k{}^i{}_j v^j_{O,0} + (H_{\beta_0})^i_j v^j_{O,0} + (h_O)^i_j v^j_{O,0}.\end{aligned} \tag{A.13}$$

All these integrals need to be evaluated at the zeroth order solution of the geodesic equation. For our experimental set-up only piecewise geodesics are considered, which to zeroth order are simply straight lines. Hence, we can use the standard affine parametrization for these geodesics

$$X(t) = (1-t)x_1 + tx_2, \quad \text{where} \quad X(0) = x_1, \quad X(1) = x_2$$

whose tangent vector is $\dot{X}(t) = x_2 - x_1 = x$. Also note that at zeroth order, the β-parallel transported image of x^i at O is just $v^i_{O,0} = x^i$. Now suppose that γ_0 is a single line segment X, whose point of origin is the end point of β_0, which is a piecewise linear path Y, whose segments are indexed by N and denoted Y_N. Then H_X contracted with arbitrary vectors A, B is given by

$$\begin{aligned}A^iB^j(H_X)_{ij} &= A^iB^j \int_X \mathrm{d}t\, x^k[\partial_k h_{[ij]} - \partial_j h_{(ki)} + \partial_i h_{(kj)}] \\ &= A^iB^j[h_{[ij]}]^{x_2}_{x_1} + 2A^{[i}B^{j]}x^k \int_X \mathrm{d}t\, \partial_i h_{(kj)}.\end{aligned}$$

The expression for H_{Y_N} is alike, with the distinction that X is replaced by Y_N and H_Y is

$$(H_Y)_{ij} = \sum_N (H_{Y_N})_{ij}. \tag{A.14}$$

The expression for $J_{X,Y}$ contracted with an arbitrary vector A is

$$\begin{aligned}A^i(J_{X,Y})_i &= -A^i \int_X \mathrm{d}t\, h_{ij}x^j + A^i \int_X^{(1)} \mathrm{d}t\, x^k[\partial_k h_{[ij]} - \partial_j h_{(ki)} + \partial_i h_{(kj)})]x^j + A^i(H_Y)_{ij}x^j + A^i(h_O)_{ij}x^j \\ &= A^i x^j (h_O)_{ij} - A^i x^j h_{[ij]}(x_1) + A^i x^j [h_{[ij]}]^{x_1}_O \\ &\quad - A^i x^j \int_X \mathrm{d}t\, h_{(ij)} + 2A^{[i}x^{j]}x^k \int_X^{(1)} \partial_i h_{(kj)} + \sum_N 2A^{[i}x^{j]}y^k_N \int_{Y_N} \mathrm{d}t\, \partial_i h_{(kj)} \\ &= A^i x^j[(h_O)_{ij} - h_{[ij]}(O)] - A^i x^j \int_X \mathrm{d}t\, h_{(ij)} + 2A^{[i}x^{j]}x^k \int_X^{(1)} \mathrm{d}t\, \partial_i h_{(kj)} + \sum_N 2A^{[i}x^{j]}y^k_N \int_{Y_N} \mathrm{d}t\, \partial_i h_{(kj)},\end{aligned}$$

where the following notation for the expressions of the contracted H_X,H_{Y_N} and J was applied

$$\int_X^{(n)} \mathrm{d}t f = \int_0^1 \mathrm{d}t_0 \int_0^{t_0} \mathrm{d}t_1 \cdots \int_0^{t_{n-1}} \mathrm{d}t_n\, f(X(t_n)), \tag{A.15}$$

$$\int_X \mathrm{d}t\, f = \int_X^{(0)} \mathrm{d}t\, f, \tag{A.16}$$

$$[f]^{x_2}_{x_1} = \int_X \mathrm{d}t\, x^i \partial_i f = f(x_2) - f(x_1). \tag{A.17}$$

Appendix B

Calculation expectation value graviton two-point function

The aim of this appendix is to compute the expectation value of the anti-commutator of the gravitational field, i.e. $\langle\{h(x)_{\mu\nu}, h(y)_{\kappa\lambda}\}\rangle$, which is related to the Poisson bracket of the gravitational field. In order to compute this, we first give a brief, relatively technical overview on how the physical phase space, on which the Poisson bracket is defined, can be constructed from the manifold of all field configurations, and we give a definition of the Poisson bracket on this phase space. Next, given this background knowledge, we give an algorithm for constructing the Poisson bracket on the physical phase space starting from the Lagrangian density. Finally, the algorithm is applied to the case we are interested in: the calculation of the expectation value of the Poisson bracket of the gravitational field from which we obtain the expectation value of the graviton two-point function.

B.1 Geometrical construction of the physical phase space from the space of field configurations

In this part, we will describe a geometrical construction of the physical phase space for Lagrangian field theories formulated on an n-dimensional spacetime M. On this spacetime, the spacetime metric $g_{\mu\nu}$ is restricted so that we can choose a time function t and a vector field t^a such that leaves Σ_t in the foliation $\mathbb{R}\times\Sigma$ with constant t are spacelike Cauchy surfaces. It should be noted that the following description holds for any Lagrangian field theory and thus is not restricted to general relativity.[1] The approach in this part is analogous to that of [21], however, we do not intend to be as complete and general, since the goal is merely to give a reasonable background for the algorithm that follows.

First, we need to define fields mathematically. We define a field (or collection of fields) ϕ as a map from the initial spacetime M to some other finite-dimensional spacetime M', that is, $\phi : M \to M'$. The manifold of all kinematically allowed field configurations satisfying appropriate asymptotic boundary conditions is denoted by $\mathcal{F}$ so that $\phi \in \mathcal{F}$.[2] In addition, we assume that there exists a functional $S[\phi] = \int_M \mathcal{L}$ where $\mathcal{L}$ is the Lagrangian density which is of the form $\mathcal{L} = \mathcal{L}(\phi, \nabla\phi, \nabla^2\phi, \ldots)$ with ∇ denoting the derivative operator on M. The field equations are obtained by varying this functional called the action and its critical points determine the physical fields. If we pick a coordinate system for M and vary the Lagrangian

[1] Albeit that when the theory is background dependent, i.e. the spacetime metric is not a dynamical variable but part of the background structure, it is also assumed that $(M, g_{\mu\nu})$ is globally hyperbolic.

[2] Note that $\phi \in \mathcal{F}$ and $\phi(x) \in M'$.

density, we obtain

$$\delta\mathcal{L} = \text{`eom'} + \nabla_\mu \theta^\mu \tag{B.1}$$

where 'eom' is shorthand for 'equations of motion' and we will call θ^μ the *symplectic potential current density* on spacetime. The latter is well-defined and while we picked a specific coordinate system to define the variation of the action, the symplectic potential current density is independent of our choice of coordinates. However, in general, it will depend on the choice for the covariant derivative operator ∇_μ. On the other hand, for a Lagrangian with no derivatives higher than second order on the field variables – which is often the case in physics – it can be shown that θ^μ is also independent on the choice for the covariant derivative operator ∇_μ. By integrating the symplectic potential current density over Σ, which is linear in the field variations $\delta\phi$ and its derivatives, we obtain the following functional

$$\theta\left[\phi, \delta\phi\right] \equiv \int_\Sigma \theta^\mu n_\mu \tag{B.2}$$

where n^μ is the outward pointing unit vector normal to the Cauchy surface Σ such that, if t^μ is tangential to Σ, $n^\mu t_\mu = 0$. If we assume that θ is continuous in the field variations of ϕ on $\mathcal{F}$, then θ defines a dual vector field on the cotangent space of $\mathcal{F}$ by the following relation

$$\theta(\phi, \delta\phi) = \theta_a \, \delta\phi^a \quad \forall\, \delta\phi^a$$

where the Roman letters for the indices indicate abstract index notation again. This notation will be used throughout for fields on $\mathcal{F}$ and objects on its tangent and cotangent bundle, respectively, $T\mathcal{F}$ and $T^*\mathcal{F}$. By taking the exterior derivative of the dual vector θ_a on $T^*\mathcal{F}$, we can define an exact (and thereby closed) 2-form on the cotangent bundle of $\mathcal{F}$

$$\omega_{ab} = (d\theta)_{ab}. \tag{B.3}$$

We refer to ω_{ab} as the *presymplectic form* on the space of all kinematically allowed field configurations. There is a reason that this form is called *pre*symplectic and not symplectic: ω_{ab} is degenerate, i.e. not invertible. This is due to the fact that the space of all field configurations $\mathcal{F}$ is unsuitable to serve as our phase space because it is "too large". Therefore, we will apply a so-called "reduction procedure" to obtain a space with a well-defined non-degenerate closed 2-form, which may then serve as our extended phase space. Let us denote

$$\begin{aligned} \omega_{\phi_0} : T_{\phi_0}\mathcal{F} &\to T^*_{\phi_0}\mathcal{F} \\ \phi_1 &\mapsto \omega_{\phi_0}(\phi_1, -), \end{aligned}$$

where ω_{ϕ_0} is the symplectic form define in eq. (B.3) evaluated at a given point ϕ_0. Naively we would like to quotient out the kernel of this map at each point on our manifold to obtain an injective map and, consequently, on finite-dimensional manifolds an invertible map. More precisely, if we relate in a point ϕ_0 on our manifold $\mathcal{F}$, ϕ_1 with ϕ_2, then in our cotangent space we can relate $\omega_{\phi_0}\,\delta\phi_1 = \omega_{\phi_0}\,\delta\phi_2$ using that $\omega_{\phi_0}\,\delta\phi_1 = \omega_{\phi_0}\,\delta\left(\phi_1 - \phi_2\right) + \omega_{\phi_0}\,\delta\phi_2$. Thus, given this equivalence relation in a point on $\mathcal{F}$, on its cotangent space ω_{ϕ_0} is injective. However, performing this at each point of our manifold to obtain a globally invertible 2-form does not guarantee smoothness. Therefore we first define certain objects globally and next, in a similar spirit as for this simple example, "quotient out the kernel" to obtain a globally well-defined invertible 2-form. For details, see [21], but we will give a rough sketch of the procedure here. We take the collection of subspaces of the tangent space to $\mathcal{F}$ that satisfy $\omega_{ab}\phi^a = 0\ \forall\, \phi^a \in T\mathcal{F}$ and assume that this collection of subspaces is a subbundle of the entire tangent space of $\mathcal{F}$. According to Frobenius theorem, we can define integral submanifolds of these subbundles. Subsequently, we define an equivalence relation on these integral submanifolds: $\phi_1 \sim \phi_2$ if and only if ϕ_1 and ϕ_2 are on the same integral submanifold. We denote the set of equivalence classes of $\mathcal{F}$ by Γ. This quotient space Γ, i.e. $\mathcal{F}/\sim$, will be the extended phase space of our theory. Note that we

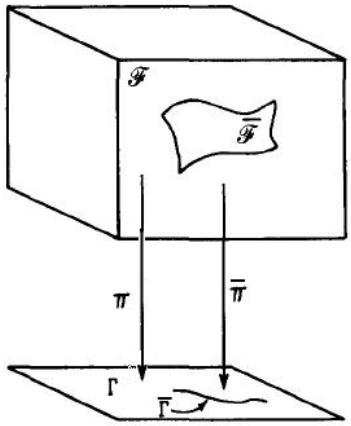

Figure B.1: The relationship between the presymplectic space of all field configurations $(\mathcal{F}, \omega)$ and the symplectic space (Γ, Ω) by the projection map π, and the reduced spaces $\bar{\mathcal{F}}$ and $\bar{\Gamma}$ are shown. Taken from [21] and edited afterwards.

explicitly call this the *extended* phase space and not the physical phase space, since this space is also still too large. How to go from this extended phase space to the physical phase space will be discussed in a bit. Assuming that we can define a manifold structure on Γ, the structure of the space of all field configurations $\mathcal{F}$ is that of a fiber bundle over Γ with its associated projection map π, where $\pi : \mathcal{F} \to \Gamma$. We can now relate the presymplectic form ω_{ab} on the space of all field configurations $\mathcal{F}$ to a well-defined non-degenerate 2-form Ω_{ab} on Γ by

$$\omega_{ab} = \pi^* \Omega_{ab}$$

where π^* is the natural pull-back map taking differential forms on Γ to differential forms on $\mathcal{F}$. This new 2-form, also known as the *symplectic form*, is now (by construction) non-degenerate. Also, as a direct consequence of the fact that ω_{ab} is closed, the symplectic form Ω_{ab} is. The property of exactness is not necessarily carried over. So (Γ, Ω_{ab}) is a symplectic manifold, which we take as the *extended phase space* of our theory. All kinematically possible states of the system are described by this space. However, we are interested in the *physical phase space*, which are all the dynamically possible states of our theory. The physical phase space is obtained by restricting the extended phase space. More formally, if we denote $\bar{\mathcal{F}}$ as the subset of $\mathcal{F}$ consisting of all solutions to the equations of motion and assume that $\bar{\mathcal{F}}$ is a submanifold of $\mathcal{F}$, we can define a submanifold $\bar{\Gamma}$ of Γ, which will be our physical phase space. The physical phase space is obtained from $\bar{\mathcal{F}}$ by the same projection map as encountered before, i.e.

$$\bar{\Gamma} = \pi\left(\bar{\mathcal{F}}\right).$$

Let $\bar{\pi}$ be the projection restricted to $\bar{\mathcal{F}}$, so $\bar{\pi} : \bar{\mathcal{F}} \to \bar{\Gamma}$, and assume that $\bar{\mathcal{F}}$ also has a fiber bundle structure over $\bar{\Gamma}$, just like $\mathcal{F}$ has over Γ. The relations between $\mathcal{F}, \Gamma, \bar{\mathcal{F}}, \bar{\Gamma}$ and their projection maps are visualized in fig. B.1. Analogously to the symplectic form on the extended phase space, we can define a symplectic form on the physical phase space via a pullback map;

$$\bar{\omega}_{ab} = \bar{\pi}^* \, \bar{\Omega}_{ab}$$

where $\bar{\omega}_{ab}$ is the restriction of ω_{ab} to $\bar{\mathcal{F}}$, and correspondingly for $\bar{\Omega}_{ab}$. Thus, the physical phase space is given by $(\bar{\Gamma}, \bar{\Omega}_{ab})$. Interestingly, although (Γ, Ω_{ab}) depends on the choice of Cauchy surface Σ in spacetime via the intermediate integral in eq. (B.2), it can be shown that $(\bar{\Gamma}, \bar{\Omega}_{ab})$ does not depend on this choice. Furthermore, it is proven in [21] that this restricted symplectic

form $\bar{\Omega}_{ab}$ is gauge-invariant. In addition, note that since $\bar{\Omega}_{ab}$ is invertible, we can define a Poisson bracket through the following relationship

$$\{\phi(x), \phi(y)\} = \bar{\Omega}^{-1}(\phi(x), \phi(y).$$

Hence, we can now given the manifold of field configurations relate this to the Poisson bracket. The method outlined is independent of one's choice of coordinates and gives a gauge-invariant result.

B.2 Algorithm to obtain the Poisson bracket on phase space from the Lagrangian

From the previous description we can construct an algorithm to find the Poisson bracket on the reduced phase space given a Lagrangian density. Given a finite-dimensional spacetime manifold M and a field theory whose Lagrangian density is known, the following step-by-step procedure applies.

1. Starting from the Lagrangian density (or equivalently, the action) derive the symplectic potential current density θ^μ, which is defined through eq.(B.1).

2. Obtain the symplectic current density ω^μ by

   $$\omega^\mu = d\theta^\mu$$

   where d denotes the exterior derivative.

3. The next step is to integrate the symplectic current density over a Cauchy surface Σ in a direction outward normal to it (denoted by the vector n^μ)

   $$\Omega = \int_\Sigma n^\mu \omega_\mu$$

   where Ω is the presymplectic form. One can choose, for instance, a timelike Cauchy hypersurface Σ_t with its normal $t^\mu = (-1, 0, 0, 0)$ so that Ω is given by $\Omega = \int_{t=0} \mathrm{d}^3\vec{x}\, t^\mu \omega_\mu(\vec{x})$, where $(t, \vec{x})$ are the usual time and spatial coordinates.

4. Restrict Ω to a space of solutions by implementing the equation of motions to obtain the symplectic form $\bar{\Omega}$. Additionally, to simplify the algebra one can fix a convenient gauge and do the calculations therein as the final result is gauge-invariant.

5. Subsequently, invert the symplectic form to get

   $$\Pi \equiv \bar{\Omega}^{-1}.$$

6. Finally, the Poisson bracket is obtained by insertion of the relevant fields into Π, e.g. $\{\phi(x), \phi(y)\} = \Pi\left(\phi(x), \phi(y)\right)$.

B.3 An application: calculation of the Poisson bracket of the gravitational field and derivation expectation value of its anti-commutator

For our action we take the Palatini action rather than the standard Einstein-Hilbert action to simplify the calculations, as they are equivalent [22]. We work in coordinates as the resulting

Poisson bracket using the algorithm in the previous part is coordinate independent. Thus, in this part we do not use abstract tensor index notation, instead Greek symbols (μ, ν,etc.) are used to denote any index that runs from 0 to 3. The Palatini action is given by

$$\begin{aligned} S &= \int \mathrm{d}^4x\, R = \int \mathrm{d}^4x\, \tilde{g}^{\mu\nu} R_{\mu\nu} \\ &= \int \mathrm{d}^4x\, \tilde{g}^{\mu\nu} \left(\partial_\alpha \Gamma^\alpha_{\mu\nu} - \partial_\nu \Gamma^\alpha_{\mu\alpha} + \Gamma^\alpha_{\nu\mu}\Gamma^\beta_{\alpha\beta} - \Gamma^\alpha_{\beta\mu}\Gamma^\beta_{\alpha\nu} \right) \end{aligned}$$

where R is the Ricci scalar, $R_{\mu\nu}$ the Ricci tensor built entirely out of $\Gamma^\alpha_{\mu\nu}$, $\tilde{g}^{\mu\nu}$ is the inverse densitized metric, $g_{\mu\nu}\tilde{g}^{\nu\lambda} = \sqrt{-g}\delta^\lambda_\mu$, g is the determinant of the metric $g_{\mu\nu}$, and $\Gamma^\alpha_{\mu\nu}$ are the Christoffel symbols encountered before. The first step is to vary the action, this gives

$$\begin{aligned} \delta S &= \frac{\delta S}{\delta \tilde{g}^{\kappa\lambda}} \delta\tilde{g}^{\kappa\lambda} + \frac{\delta S}{\delta \Gamma^\kappa_{\lambda\sigma}} \delta\Gamma^\kappa_{\lambda\sigma} \\ &= \text{`eom'} + \int \mathrm{d}^4x\, \partial_\alpha \left(\tilde{g}^{\mu\nu}\delta\Gamma^\alpha_{\mu\nu} - \tilde{g}^{\mu\alpha}\delta\Gamma^\nu_{\mu\nu} \right), \end{aligned}$$

thus, $\theta^\alpha = \tilde{g}^{\mu\nu}\delta\Gamma^\alpha_{\mu\nu} - \tilde{g}^{\mu\alpha}\delta\Gamma^\nu_{\mu\nu}$. Second, we obtain the presymplectic potential current density

$$\omega^\alpha = \delta\theta^\alpha = \delta\tilde{g}^{\mu\nu} \wedge \delta\Gamma^\alpha_{\mu\nu} - \delta\tilde{g}^{\mu\alpha} \wedge \delta\Gamma^\nu_{\mu\nu},$$

where the variational derivative δ is applied according to the usual rules of an exterior derivative, making ω^α a spacetime current density and a 2-form on the infinite dimensional space of field configurations. Third, we find the presymplectic form by integrating over a Cauchy surface. As our Cauchy surface, we take the timelike hypersurface as suggested in step 3 with the associated normal vector $t^\mu = (-1, 0, 0, 0)$.

$$\begin{aligned} \Omega &= \int_{t=0} \mathrm{d}^3x\, t_\mu \omega^\mu \\ &= \int_{t=0} \mathrm{d}^3x\, (\delta\tilde{g}^{\mu\nu} \wedge \delta\Gamma^0_{\mu\nu} - \delta\tilde{g}^{\mu 0} \wedge \delta\Gamma^\nu_{\mu\nu}) \end{aligned} \tag{B.4}$$

Fourth, we need to restrict Ω to an unique space of solutions. Additionally, thus far, we have taken the spacetime metric $g_{\mu\nu}$ to be arbitrary. However, from this point on, we restrict ourselves to linearized gravity as we are ultimately interested in calculating the expectation value of the graviton's two point function, i.e. we take $g_{\mu\nu} = \eta_{\mu\nu} + h_{\mu\nu} + \mathcal{O}(h^2)$ and accordingly

$$\Gamma^\alpha_{\mu\nu} = \frac{1}{2}\eta^{\alpha\beta} \left(\partial_\mu h_{\beta\mu} + \partial_\nu h_{\beta\mu} - \partial_\beta h_{\mu\nu} \right) + \mathcal{O}(h^2), \tag{B.5}$$

$$\tilde{g}^{\mu\nu} = \eta^{\mu\nu} - h^{\mu\nu} + \frac{1}{2}\eta^{\mu\nu} h^\alpha{}_\alpha + \mathcal{O}(h^2), \tag{B.6}$$

where indices are raised using $\eta^{\mu\nu}$. We need to specify a full gauge which is given by the Lorentz, radiation, trace gauge, i.e. the following restrictions need to hold

$$\begin{aligned} &h^\mu{}_\mu = 0, \\ &t_\mu h^{\mu\nu} = h^{0\nu} = 0, \\ &\partial^i h_{ij} = 0. \end{aligned}$$

The equations of motion are $\partial^\lambda\partial_\lambda\, h_{\mu\nu} = \Box\, h_{\mu\nu}$, whose solutions are

$$h_{\mu\nu}(x) = \int \frac{\mathrm{d}^3k}{(2\pi)^3} e^{ikx} \left(P^1_{\mu\nu}(k)\{\alpha^+_1(k)e^{-ikt} + \alpha^-_1(k)e^{ikt}\} + P^2_{\mu\nu}(k)\{\alpha^+_2(k)e^{-ikt} + \alpha^-_2(k)e^{ikt}\right)$$

where $\alpha^{\pm}_{1/2}$ are constants depending on k and the polarization factors $P^1_{\mu\nu}$ and $P^2_{\mu\nu}$ need to satisfy

$$\begin{aligned}
&\eta^{\mu\nu}P^i_{\mu\nu} = 0,\\
&t^\mu P^i_{\mu\nu} = P^i_{0\nu} = 0,\\
&k^\mu P^i_{\mu\nu} = 0,\\
&P^i_{\mu\nu}(P^{\mu\nu})^j = \delta^{ij},
\end{aligned} \tag{B.7}$$

for $i = 1, 2$. The first three conditions are directly related to the gauge-fixing and the latter is a result from requiring orthogonality of the polarization factors. In the final expression for the Poisson bracket, $P^1_{\mu\nu}P^1_{\lambda\kappa} + P^2_{\mu\nu}P^2_{\lambda\kappa}$ appears, which we will refer to as the *projected identity*. To find this tensor, we use all the restrictions above, use as a basis $\eta_{\mu\nu}, t_\mu, k_\mu$ and require that it is symmetric under exchange of indices $(\mu\nu) \leftrightarrow (\kappa\lambda)$, $\mu \leftrightarrow \nu$ and $\kappa \leftrightarrow \lambda$. So here we will take a slight tangent to find the projected identity. Using the basis and symmetry requirements, we know that the projected identity should be of the following form

$$\begin{aligned}
P^1_{\mu\nu}P^2_{\kappa\lambda} =& \frac{1}{2}\left(\eta_{\mu\kappa}\eta_{\nu\lambda} + \eta_{\mu\lambda}\eta_{\nu\kappa}\right) + A\,\eta_{\mu\nu}\eta_{\kappa\lambda} + B\left(\eta_{\mu\nu}k_\kappa k_\lambda + \eta_{\kappa\lambda}k_\mu k_n u\right)\\
&+ C\left(\eta_{\mu\nu}k_\nu k_\lambda + \eta_{\nu\kappa}k_\mu k_\lambda + \eta_{\mu\lambda}k_\nu k_\kappa + \eta_{\nu\lambda}k_\mu k_\kappa\right) + D\left(\eta_{\mu\nu}t_\kappa t_\lambda + \eta_{\kappa\lambda}t_\mu k_n u\right)\\
&+ E\left(\eta_{\mu\nu}t_\nu t_\lambda + \eta_{\nu\kappa}t_\mu t_\lambda + \eta_{\mu\lambda}t_\nu t_\kappa + \eta_{\nu\lambda}t_\mu t_\kappa\right) + F\left(\eta_{\mu\nu}k_\kappa t_\lambda + \eta_{\mu\nu}k_\lambda t_\kappa + \eta_{\kappa\lambda}k_\mu t_\nu + \eta_{\kappa\lambda}k_\nu t_\mu\right)\\
&+ G\left(\eta_{\mu\kappa}k_\nu t_\lambda + \eta_{\nu\kappa}k_\mu t_\lambda + \eta_{\mu\lambda}k_\nu t_\kappa + \eta_{\mu\lambda}k_\mu t_\kappa\right) + H\left(\eta_{\mu\kappa}k_\lambda t_\nu + \eta_{\nu\kappa}k_\lambda t_\mu + \eta_{\mu\lambda}t_\nu k_\kappa + \eta_{\nu\lambda}t_\mu k_\kappa\right)\\
&+ I\,k_\mu k_\nu k_\kappa k_\lambda + J\left(k_\mu k_\nu k_\kappa t_\lambda + k_\mu k_\nu k_\lambda t_\kappa + k_\mu k_\kappa k_\lambda t_\nu + k_\nu k_\kappa k_\lambda t_\mu\right) + K\left(k_\mu k_\nu t_\kappa t_\lambda + k_\kappa k_\lambda t_\mu t_\nu\right)\\
&+ L\left(k_\mu k_\kappa t_\nu t_\lambda + k_\mu k_\lambda t_\nu t_\kappa + k_\nu k_\kappa t_\mu t_\lambda + k_\nu k_\lambda t_\mu t_\kappa\right) + M\left(k_\mu t_\nu t_\kappa t_\lambda + k_\nu t_\mu t\kappa t_\lambda + k_\kappa t_\mu t_\nu t_\lambda + k_\lambda t_\mu t_\nu t_\kappa\right)\\
&+ N\,t_\mu t_\nu t_\kappa t_\lambda
\end{aligned}$$

where the capital letters are constants that will be fixed by the restrictions in eq. (B.7). We have 14 constants; the trace condition gives four independent constraints and projection onto t^μ and k^μ each give ten constraints amounting to a total of 24 constraints. Fortunately, some contraints are redundant and the system is exactly solvable. Having set $t^2 = 1$, we obtain the following expressions for the constants

$$\begin{aligned}
A &= -\frac{1}{2}, & H &= \frac{-kt}{2\left(k^2 + (k\cdot t)^2\right)},\\
B &= \frac{1}{2\left(k^2 + (k\cdot t)^2\right)}, & I &= \frac{1}{2\left(k^2 + (k\cdot t)^2\right)^2},\\
C &= -\frac{1}{2\left(k^2 + (k\cdot t)^2\right)}, & J &= \frac{kt}{2\left(k^2 + (k\cdot t)^2\right)^2},\\
D &= -\frac{k^2}{2\left(k^2 + (k\cdot t)^2\right)}, & K &= \frac{k^2 + 2(k\cdot t)^2}{2\left(k^2 + (k\cdot t)^2\right)^2},\\
E &= \frac{k^2}{2\left(k^2 + (k\cdot t)^2\right)}, & L &= -\frac{k^2}{2\left(k^2 + (k\cdot t)^2\right)^2},\\
F &= \frac{kt}{2}\frac{1}{\left(k^2 + (k\cdot t)^2\right)}, & M &= -\frac{k^2(k\cdot t)}{2\left(k^2 + (k\cdot t)^2\right)^2},\\
G &= -\frac{kt}{2}\frac{1}{\left(k^2 + (k\cdot t)^2\right)}, & N &= \frac{k^4}{2\left(k^2 + (k\cdot t)^2\right)^2}.
\end{aligned}$$

The resulting projected identity is rather long and complicated, conveniently, there are some simplifications that can de made. Since $h_{\mu\nu}$ has gauge degrees of freedom of the form $k_{(\mu}\zeta_{\nu)}$, all terms that have a similar form can consequently be gauged away when calculating observables. Additionally, the projected identity will appear in the graviton two-point function within an

integral over k together with $\delta^{(4)}(k^2)$, hence all terms that are proportional to k^2 will vanish. Ergo, the only non-vanishing constant is $A = -\frac{1}{2}$ and the projected identity for calculating observables is

$$P^1_{\mu\nu}P^1_{\kappa\lambda} + P^2_{\mu\nu}P^2_{\kappa\lambda} = \frac{1}{2}\left(\eta_{\mu\kappa}\eta_{\nu\lambda} + \eta_{\mu\lambda}\eta_{\nu\kappa} - \eta_{\mu\nu}\eta_{\kappa\lambda}\right) \equiv \frac{1}{2}\eta_{\mu\nu,\kappa\lambda} \tag{B.8}$$

If we implement the gauge conditions and substitute the expression for the Christoffel symbol to linear order into the expression for the presympletic form in eq. (B.4), we get

$$\bar{\Omega} = \frac{1}{2}\int_{t=0} \mathrm{d}^3x\ \delta h^{\mu\nu} \wedge \delta\partial_0 h_{\mu\nu}$$

Inserting the solution for the gravitational field gives

$$\begin{aligned}\bar{\Omega} =& \frac{1}{2}\int_{t=0}\mathrm{d}^3x \int\frac{\mathrm{d}^3k}{(2\pi)^3}\int\frac{\mathrm{d}^3k'}{(2\pi)^3}\,\delta\left(e^{ikx}\left((P^1)^{\mu\nu}(k)\{\alpha_1^+(k)e^{-ikt} + \alpha_1^-(k)e^{ikt}\}+\right.\right.\\ &\left.(P^2)^{\mu\nu}(k)\{\alpha_2^+(k)e^{-ikt} + \alpha_2^-(k)e^{ikt}\}\right) \wedge\ \delta\left(ik'e^{ik'x}\left(P^1_{\mu\nu}(k')\{-\alpha_1^+(k')e^{-ik't} + \alpha_1^-(k')e^{ik't}\}\right.\right.\\ &\left.\left.+\ P^2_{\mu\nu}(k')\{-\alpha_2^+(k')e^{-ik't} + \alpha_2^-(k')e^{ik't}\}\right)\right)\end{aligned}$$

Performing the integration over x gives a delta-function $\delta(k+k')$ and the ensuing integration over k' yields

$$\begin{aligned}\bar{\Omega} =& \frac{1}{2}\int_{t=0}\frac{\mathrm{d}^3k}{(2\pi)^3}\,\delta\left((P^1)^{\mu\nu}(k)\{\alpha_1^+(k)e^{-ikt} + \alpha_1^-(k)e^{ikt}\} + (P^2)^{\mu\nu}(k)\{\alpha_2^+(k)e^{-ikt} + \alpha_2^-(k)e^{ikt}\}\right)\\ &\wedge\,\delta\left(P^1_{\mu\nu}(-k)\{\alpha_1^+(-k)e^{ikt} - \alpha_1^-(-k)e^{-ikt}\} + P^2_{\mu\nu}(-k)\{\alpha_2^+(-k)e^{ikt} - \alpha_2^-(-k)e^{-ikt}\}\right)\end{aligned} \tag{B.9}$$

From the requirement that the gravitational field is real, i. e. $h^*_{\mu\nu}(x) = h_{\mu\nu}(x)$, and the relations $P^1_{\mu\nu}(-k) = P^1_{\mu\nu}(k)$ and $P^2_{\mu\nu}(-k) = -P^2_{\mu\nu}(k)$,[3] we obtain the following identities for $\alpha_1^\pm$ and $\alpha_2^\pm$

$$\begin{aligned}\alpha_1^+(k) &= \alpha_1^{-*}(-k),\\ \alpha_1^-(k) &= \alpha_1^{+*}(-k),\\ \alpha_2^+(k) &= -\alpha_2^{-*}(-k),\\ \alpha_2^-(k) &= -\alpha_2^{+*}(-k).\end{aligned}$$

The expression for the symplectic form in eq. (B.9) can now be massaged using the relations for the α's above. In addition, to simplify the expression we take $\vec{k}$ in the z-direction and integrate only over the upper half plane; to obtain the correct result integration over the lower half plane is added by hand. Furthermore, writing out the wedge-product, applying the orthogonality conditions of the polarization factors and setting $t = 0$ everywhere gives

$$\bar{\Omega} = \int_{\mathbb{R}^3_+}\frac{\mathrm{d}^3k}{(2\pi)^3}ik\left(-\delta\alpha_1^+ \wedge \delta\alpha_1^{+*} + \delta\alpha_1^- \wedge \delta\alpha_1^{-*} - \delta\alpha_2^+ \wedge \delta\alpha_2^{+*} + \delta\alpha_2^- \wedge \delta\alpha_2^{-*}\right)$$

where for notational clarity the k dependence has been omitted since now all dependence is on $+k$. The fifth step is to invert the symplectic form, to obtain Π

$$\Pi = \int_{\mathbb{R}^3_+}\mathrm{d}^3k\frac{(2\pi)^3}{ik}\left(-\partial\alpha_1^+ \wedge \partial\alpha_1^{+*} + \partial\alpha_1^- \wedge \partial\alpha_1^{-*} - \partial\alpha_2^+ \wedge \partial\alpha_2^{+*} + \partial\alpha_2^- \wedge \partial\alpha_2^{-*}\right)$$

[3] These relations are obvious if one takes

$$\begin{aligned}P^1_{\mu\nu} &\sim \text{“}\theta\theta + \phi\phi''\\ P^2_{\mu\nu} &\sim \text{“}\theta\phi + \phi\theta''\end{aligned}$$

Lastly, the Poisson bracket of the gravitational field is obtained from $\Pi\left(h(x)_{\mu\nu}, h(y)_{\kappa\lambda}\right)$. Applying the following identities

$$\begin{aligned}
&\partial_{\alpha_1^+(k)}\alpha_1^+(q) = \delta(k-q),\\
&\partial_{\alpha_1^+(k)} \wedge \partial_{\alpha_1^+(k)^*}\left(\alpha_1^+(p), \alpha_1^-(q)\right) = \delta(k-p)\delta(k+q),\\
&\partial_{\alpha_1^+(k)} \wedge \partial_{\alpha_1^+(k)^*}\left(\alpha_1^+(p), \alpha_1^+(q)\right) = 0,\\
&\partial_{\alpha_1^-(k)} \wedge \partial_{\alpha_1^-(k)^*}\left(\alpha_1^+(p), \alpha_1^-(q)\right) = -\delta(k-p)\delta(k+q),\\
&\partial_{\alpha_2^+(k)} \wedge \partial_{\alpha_2^+(k)^*}\left(\alpha_2^+(p), \alpha_2^-(q)\right) = -\delta(k-p)\delta(k+q),\\
&\partial_{\alpha_2^-(k)} \wedge \partial_{\alpha_2^-(k)^*}\left(\alpha_2^+(p), \alpha_2^-(q)\right) = \delta(k-p)\delta(k+q),
\end{aligned}$$

and properly rewriting gives

$$\begin{aligned}
\{h(x)_{\mu\nu}, h(y)_{\kappa\lambda}\} &= 2\pi \int \frac{\mathrm{d}^4k}{(2\pi)^4} \frac{\delta^{(4)(k^2)}}{i}\left(P^1_{\mu\nu}P^1_{\kappa\lambda} + P^2_{\mu\nu}P^2_{\kappa\lambda}\right) e^{ik(x-y)}\mathrm{sgn}(\omega)\\
&= \frac{1}{2}\,2\pi \int \frac{\mathrm{d}^4k}{(2\pi)^4} \frac{\delta^{(4)}(k^2)}{i}\eta_{\mu\nu,\kappa\lambda}e^{ik(x-y)}\mathrm{sgn}(\omega)
\end{aligned} \tag{B.10}$$

where $\omega = k^0$ and $\mathrm{sgn}(x)$ is the sign-function. The only thing left is to obtain the full expression for the expectation value of anti-commutator of the gravitational field with respect to the Fock vacuum. This is done using two relations: (i) $[A,B]_- = i\hbar\{A,B\}$, which relates the anti-commutator with the Poisson bracket, and (ii) a relation between the anti-commutator and commutator Green functions of quantum simple harmonic oscillators. This second relation is also applicable for the gravitational field, since, as discussed before, a linear field theory is a collection of coupled harmonic oscillators. The relation between the two Green functions with frequency $\omega > 0$ and position operator $\hat{x}(t)$ is

$$\langle[\hat{x}(t), \hat{x}(s)]_+\rangle = (\Omega_+ - \Omega_-)[\hat{x}(t), \hat{x}(s)]_- \tag{B.11}$$

where $\langle\ldots\rangle$ denotes the expectation value with respect to the ground state, the commutator and anti-commutator are distinguished by the $\pm$-sign and we defined the positive and negative frequency projection operators as

$$\begin{aligned}
&\Omega_+ e^{-i\omega t} = e^{-i\omega t}, && \Omega_- e^{-i\omega t} = 0,\\
&\Omega_+ e^{+i\omega t} = 0, && \Omega_- e^{+i\omega t} = e^{+i\omega t}.
\end{aligned}$$

Thus, using relation (i) between the commutator and Poisson bracket and relation (ii) between the commutator and anti-commutator Green functions, the expectation value of the anti-commutator of the gravitational field is

$$\langle[h(x)_{\mu\nu}, h(y)_{\kappa\lambda}]_+\rangle = i\hbar(\Omega_+ - \Omega_-)\{h(x)_{\mu\nu}, h(y)_{\kappa\lambda}\}$$

Inserting eq. (B.10) into this expression kills the $\mathrm{sgn}(\omega)$ term. Evaluation of the remaining

integral is carried out below

$$\begin{aligned}
\frac{\hbar}{2}2\pi\int\frac{\mathrm{d}^4k}{(2\pi)^4}\,e^{ik\cdot x}\delta(\omega^2-k^2) &= \frac{\hbar}{2}\frac{1}{(2\pi)^3}\int\mathrm{d}\omega\int\mathrm{d}\vec{k}\,e^{-i\omega t+i\vec{k}\cdot\vec{x}}\delta(\omega^2-k^2)\\
&= \frac{1}{(2\pi)^2}\int_0^\infty\mathrm{d}k\,k^2\frac{(e^{-ikt}+e^{ikt})}{2k}\frac{(e^{ikr}-e^{-ikr})}{ikr}\\
&= \frac{\hbar}{2}\frac{1}{(2\pi)^2}\int_0^\infty\mathrm{d}k\,\frac{[e^{ik(r-t+i0)}+e^{ik(r+t+i0)}-e^{-ik(r-t-i0)}-e^{-ik(r+t-i0)}]}{2ir}\\
&= \frac{\hbar}{2}\frac{1}{(2\pi)^2}\frac{(-i)}{2r}\left[-\frac{1}{i(r-t+i0)}-\frac{1}{i(r+t+i0)}-\frac{1}{i(r-t-i0)}-\frac{1}{i(r+t-i0)}\right]\\
&= \frac{\hbar}{2}\frac{1}{(2\pi)^2}\frac{1}{2r}\left(P\left[\frac{2}{r-t}\right]+P\left[\frac{2}{r+t}\right]\right)\\
&= \frac{\hbar}{2}\frac{1}{2\pi^2}P\left[\frac{1}{-t^2+\vec{x}^2}\right],
\end{aligned}$$

where it is clear from the context whether k is the four vector or the absolute value of the three vector. Further note that result of the above Fourier transform is a distribution, namely, the symbol P shows that we have to use the Cauchy principal value of $1/(x-y)^2$.

At last, the expectation value of the graviton two-point function is

$$\langle\{h(x)_{\mu\nu},h(y)_{\kappa\lambda}\}\rangle=\eta_{\mu\nu,\kappa\lambda}\,\frac{4\ell_p^2}{\pi}P\left[\frac{1}{(x-y)^\mu(x-y)_\mu}\right]=\eta_{\mu\nu,\kappa\lambda}\,\frac{4\ell_p^2}{\pi}P\left[\frac{1}{(x-y)^2}\right],$$

where we changed notation: the anti-commutator is no longer denoted by $[\ldots]_+$ but by curly brackets. This is done to match the notation in the remainder of this thesis. In addition, we reinserted all dimensionful constants using that originally in the Palatini action there was a factor $\frac{\hbar}{16\pi\ell_p^2}$.

To find this constant $\alpha=\frac{\hbar}{16\pi\ell_p^2}$ in the Palatini action ($S_P=\int\mathrm{d}x\,\mathcal{L}_P=\alpha\int\mathrm{d}x\,\sqrt{-g}\,R$), we used that in the weak field Newtonian limit, the Einstein field equations should reproduce

$$G_{\mu\nu}=8\pi T_{\mu\nu}$$

where $G_{\mu\nu}$ is the Einstein tensor and $T_{\mu\nu}$ the stress-energy-momentum density tensor of matter. The Einstein field equations are obtained by varying the total action with respect to the inverse metric, i.e.

$$\frac{\delta S_P}{\delta g^{\mu\nu}}=-\frac{\delta S_M}{\delta g^{\mu\nu}}\tag{B.12}$$

where subscripts refer to the gravitational and matter action. To fix the constant α let us take a simple action for matter: we consider the action for a grain of dust whose stress energy-density is given by $T_{\mu\nu}=\frac{G}{c^2}\rho u_\mu u_\nu$, where ρ is the rest mass density of the grain of dust supported on its worldline $\gamma(\tau)$ with τ its proper time and u_μ is the unit velocity vector $\frac{d}{d\tau}\gamma(\tau)$ [5]. The rest mass density can thus be written as $\rho=m\int\mathrm{d}\tau\,\frac{\delta^4(x-\gamma(\tau))}{\sqrt{-g}}$. The constants in the action for a grain of dust are fixed by two requirements: (i) it needs to reproduce the known non-relativistic limit and (ii) the quantum commutation relation $[x,p]=i\hbar$ which can be obtained from the action should hold. This gives for the matter action S_M

$$\begin{aligned}
S_M &= -mc\int\mathrm{d}\tau\,\sqrt{-\dot\gamma^\mu(\tau)\dot\gamma^\nu(\tau)g_{\mu\nu}}\\
&= -mc\int\mathrm{d}x\int\mathrm{d}\tau\,\delta^4(x-\gamma(\tau))\sqrt{-\dot\gamma^\mu(\tau)\dot\gamma^\nu(\tau)g_{\mu\nu}}.
\end{aligned}$$

Varying this action with respect to the inverse metric yields

$$\begin{aligned}\frac{\delta S_M}{\delta g^{\mu\nu}} &= -mc\int \mathrm{d}\tau\, \delta^4(x-\gamma(\tau))\frac{1}{2}\frac{-\dot\gamma^\sigma\dot\gamma^\phi}{\sqrt{-\dot\gamma^\kappa(\tau)\dot\gamma^\lambda(\tau)g_{\kappa\lambda}}}(-g_{\sigma\mu}g_{\phi\nu})\\ &= -\frac{c}{2}\sqrt{-g}\,\rho u_\mu u_\nu = -\frac{c^3}{2G}\sqrt{-g}\,T_{\mu\nu},\end{aligned}$$

where going from the first to the second line the definition for the mass density is applied. Variation of the gravitational action gives $\alpha\sqrt{-g}G_{\mu\nu}$ and in line with eq. (B.12) we obtain

$$\alpha\sqrt{-g}G_{\mu\nu} = \frac{c^3}{2G}\sqrt{-g}\,T_{\mu\nu} \xrightarrow{\text{'Newtonian limit'}} \frac{c^3}{2G\alpha} = 8\pi.$$

Hence, the constant in front of the Palatini action is indeed given by $\alpha = \frac{c^3}{16\pi G} = \frac{\hbar}{16\pi\ell_p^2}$.

Appendix C

Explicit calculation by hand

In this appendix, we calculate for a very specific case the smeared integral $\tilde{I}_0^{00}$ by hand. In particular, we consider the integral along two parallel single integrated null-like line segments. This case is chosen as it is a fairly simple calculation with not too many intermediate steps. We use the same notation as in ch. 5. This calculation serves as a partial check on our final result and indeed all results in this appendix are reproduced by our computer calculations.

We are to calculate the following integral along two parallel null-like line segments

$$\tilde{I}_0^{00} = \int \mathrm{d}^4 z \int_0^1 \mathrm{d}s \int_0^1 \mathrm{d}t\, P \frac{1}{(x(s) - y(t) - z)^2} g(z_\perp^2)\delta(u \cdot z).$$

For any null-like line segment $x(s)$ confined to the $(u, \hat{u})-$plane, we can take $x(s) = s\,\lambda(u - \hat{u})$ with λ denoting the length of the null segment, and similarly for $y(t) = t\,\lambda(u - \hat{u})$, so that $x^2 = y^2 = 0$. To rewrite the denominator the following identities are useful

$$\begin{aligned} z \cdot x &= -s\lambda(c - T), \\ ((s-t)x - z)^2 &= z^2 + 2(t-s)x \cdot z + (t-s)^2 x^2. \end{aligned}$$

Parametrizing the integral in the same manner as is done in ch. 5 and rearranging the denominator gives

$$\tilde{I}_0^{00} = \underbrace{-\int_0^{2\pi} \mathrm{d}\phi \int_{-\infty}^{\infty} \mathrm{d}T \delta^{(d)}(-T) \int_0^{\infty} \mathrm{d}R\, R\, g(R^2)}_{\text{part II}} \underbrace{\int_0^1 \mathrm{d}s \int_0^1 \mathrm{d}t \int_{-R}^{R} \mathrm{d}c P \frac{1}{R^2 - T^2 - 2\lambda(t-s)(c-T)}}_{\text{part I}}.$$

To compute this integral, we follow the same logic that the computer algebra uses. We calculate 'part I' first, which amounts to performing the integration over c, s and t, subsequently, we compute 'part II' which entails integration over ϕ, R and T. Thus, we start by integration over c

$$\int_{-R}^{R} \mathrm{d}c \frac{1}{R^2 - T^2 - 2\lambda(t-s)(c-T)} = \left[-\frac{1}{2\lambda(t-s)} \left(\ln|c - T| + \ln|c + T - 2\lambda(t-s)| \right) \right]_{-R}^{R}. \tag{C.1}$$

In the remaining part, we drop the boundary signs for c. Next, integration along s and t is performed. The first term in eq. (C.1) gives

$$\int \mathrm{d}s \int \mathrm{d}t - \frac{\ln|c - T|}{2\lambda(t-s)} = -\frac{1}{2\lambda} \ln|c - T| \left[[-(t-s)\left(\ln|t-s| - 1\right)] \right],$$

where the square brackets indicate that the boundaries of s and t still need to be inserted. These boundaries correspond to the four vertices in fig. 5.1. The second term in eq. (C.1) yields

$$\begin{aligned}\int \mathrm{d}s \int \mathrm{d}t - \frac{\ln|c+T-2\lambda(t-s)|}{2\lambda(t-s)} &= -\frac{\ln|c+T|}{2\lambda}\left(\int \mathrm{d}s \int \mathrm{d}t \frac{1}{t-s}\right) - \frac{1}{2\lambda}\int \mathrm{d}s \int \mathrm{d}t \frac{\ln|1-\frac{2\lambda(t-s)}{c+T}|}{t-s} \\ &= -\frac{\ln|c+T|}{2\lambda}\left[[-(t-s)\left(\ln|t-s|-1\right)]\right] - \frac{1}{2\lambda}\left[\int \mathrm{d}s\, L\left(\frac{2\lambda(t-s)}{c+T}\right)\right] \\ &= -\frac{\ln|c+T|}{2\lambda}\left[[-(t-s)\left(\ln|t-s|-1\right)]\right] \\ &\quad - \frac{1}{2\lambda}\left[\left[-(t-s) + \left(t-s-\frac{c+T}{2\lambda}\right)\ln\left|1-\frac{2\lambda(t-s)}{c+T}\right|\right.\right. \\ &\quad \left.\left. +(t-s)L\left(\frac{2\lambda(t-s)}{c+T}\right)\right]\right].\end{aligned}$$

After combining the two equations again and extracting the logarithmic divergences from the dilogarithm by applying eq. (5.17), we obtain

$$\begin{aligned}&-\frac{1}{2\lambda}\left[\left[-\left(\ln|c+T|+\ln|c-T|\right)(t-s)\left(\ln|t-s|-1\right)-(t-s)+\left((t-s)-\frac{c+T}{2\lambda}\right)\ln\left|1-\frac{2\lambda(t-s)}{c+T}\right|\right.\right. \\ &\left.\left.-(t-s)L\left(\frac{c+T}{2\lambda(t-s)}\right)-\frac{t-s}{2}(\ln|\frac{c+T}{2\lambda(t-s)}|)^2+\frac{\pi^2}{12}(t-s)+\frac{\pi^2}{4}(t-s)\mathrm{sgn}\left(\frac{c+T}{2\lambda(t-s)}\right)\right]\right].\end{aligned}$$

Evaluating this result at the boundaries $(s,t)=(0,0)$ and $(s,t)=(1,1)$ which correspond to the z_{11} and z_{22} vertices gives zero. The $(s,t)=(1,0)$ and $(s,t)=(0,1)$ boundaries which map to the z_{12} and z_{21} vertices give a non-zero result given by

$$-\frac{1}{2\lambda}\left(\frac{\ln|1+\frac{2\lambda}{c+T}|}{\ln|1-\frac{2\lambda}{c+T}|}+\frac{c+T}{2\lambda}\ln\left|1-\left(\frac{2\lambda}{c+T}\right)^2\right|+L\left(\frac{c+T}{2\lambda}\right)-L\left(-\frac{c+T}{2\lambda}\right)-\frac{\pi^2}{2}\mathrm{sgn}\left(\frac{c+T}{2\lambda}\right)\right).$$

Expanding this for small $c+T$ yields

$$-\frac{1}{2\lambda}\left(2\frac{c+T}{\lambda}-\frac{c+T}{\lambda}\ln|\frac{c+T}{2\lambda}|-\frac{\pi^2}{2}\mathrm{sgn}\left(\frac{c+T}{2\lambda}\right)\right)+\mathcal{O}((c+T)^2),$$

where we recall that the summation over $c=\pm R$ still needs to be performed. Now 'part I' has been carried out, we are left to evaluate 'part II'. Integration over ϕ and T is trivial and using the definition in eq. (5.19), the result is

$$\tilde{I}_0^{00}=\frac{\pi}{\lambda^2}\left(4-2\ln|\mu|+2\ln|2\lambda|-\frac{\pi^2\,\lambda}{\mu}\right)+\mathcal{O}(\mu^0),$$

where simple sanity checks such as the argument of a logarithm needs to be dimensionless and each term should have the same length dimension (viz. -2) are satisfied.[1]

This calculation can also be used to calculate terms with one or two derivatives on the smearing function. However, these calculations are slightly more involved since now also terms proportional to c and c^2 appear in 'part I' and integration by parts needs to be performed in 'part II' (sometimes even multiple times). The results of the calculation for the remaining integrals are quoted here without any intermediate steps and are also all reproduced by the computer algebra. The calculation for one derivative on the smearing function gives for tensor basis $\{u\}$

[1]This calculation has also been performed in two different ways (one other in position space and one in momentum space). The results of all these calculations agree. Thus, we can be confident that this result is correct.

and $\{\hat{u}\}$ both zero after evaluating the integration over c at its boundaries. The results for two derivatives on the smearing function for each tensor basis element are

$$\{uu\} \qquad \frac{\pi}{\lambda^2}\left(-\frac{2}{\mu^2}+\pi^2\,\lambda\,g(0)\right)+\mathcal{O}(\mu^0),$$

$$\{u\hat{u}+\hat{u}u\} \qquad \frac{\pi}{\lambda^2}\left(-\frac{4}{\mu^2}+\frac{8\ln|\mu|}{\mu^2}-\frac{8\ln|2\lambda|}{\mu^2}+2\pi^2\,\lambda\,g(0)\right)+\mathcal{O}(\mu^0),$$

$$\{\hat{u}\hat{u}\} \qquad \frac{\pi}{\lambda^2}\left(\frac{10}{\mu^2}+\frac{12\ln|\mu|}{\mu^2}-\frac{12\ln|2\lambda|}{\mu^2}+\pi^2\,\lambda\,g(0)\right)+\mathcal{O}(\mu^0),$$

$$\{\delta_\perp\} \qquad \frac{\pi}{\lambda^2}\left(-\frac{4}{\mu^2}+\frac{4\ln|\mu|}{\mu^2}-\frac{4\ln|2\lambda|}{\mu^2}\right)+\mathcal{O}(\mu^0).$$

Acknowledgements

I would like to thank Igor for his active involvement in this project. He allowed me to learn more about the more conservative approach to quantum gravity, but was never hesitant to teach me about other approaches. In addition, I would like to thank him for the more practical aspects of this research project such as help with debugging code and the extensive feedback on the write-up of this thesis while traveling himself. Also, I would like to thank professor Renate Loll for the interest she showed in my progress. Michael, Jules, Gertjan, Niels, Renée and my other fellow students in the master student room, a thank you for you too for the wonderful atmosphere, the great discussions, proofreading (parts of) my thesis and helping with LaTeX.

References

[1] R. P. Woodard, "How far are we from the quantum theory of gravity?," *Reports on Progress in Physics*, vol. 72, 2009.

[2] S. Carlip, "Quantum gravity : a progress report," *Reports on Progress in Physics*, no. March, 2001.

[3] I. Khavkine, "Quantum astrometric observables I: time delay in classical and quantum gravity," *Physical Review D*, vol. 85, no. 12, 2012.

[4] A. C. Hirshfeld and P. Henselder, "Deformation quantization in the teaching of quantum mechanics," *American Journal of Physics*, vol. 70, no. 5, p. 537, 2002.

[5] R. M. Wald, *General relativity*. University Of Chicago Press, 1984.

[6] W. Pauli, *General principles of quantum mechanics*. Springer, New York, 1980.

[7] J. Hilgevoord, "Time in quantum mechanics," *American Journal of Physics*, vol. 70, no. 3, p. 301, 2002.

[8] S. Blanes, F. Casas, J. Oteo, and J. Ros, "The Magnus expansion and some of its applications," *Physics Reports*, vol. 470, pp. 151–238, Jan. 2009.

[9] H. Salecker and E. P. Wigner, "Quantum limitations of the measurement of space-time distances," *Physical Review*, vol. 109, pp. 571–577, Jan 1958.

[10] S. Ohlmeyer, *The measurement of length in linear quantum gravity*. PhD thesis, University of Hamburg, 1997.

[11] H. Ford, "Gravitons and light cone fluctuations," *Physical Review D*, vol. 51, no. 4, 1995.

[12] H. Yu and L. H. Ford, "Light-cone fluctuations in flat spacetimes with nontrivial topology," vol. 60, no. April, 1999.

[13] J. Borgman and L. Ford, "Effects of stress tensor fluctuations upon focusing," *Physical Review D*, vol. 70, pp. 1–14, Sept. 2004.

[14] R. Thompson and L. Ford, "Spectral line broadening and angular blurring due to spacetime geometry fluctuations," *Physical Review D*, vol. 74, pp. 1–12, July 2006.

[15] N. C. Tsamis and R. Woodard, "Physical Green's functions in quantum gravity," *Annals of Physics*, vol. 251, 1992.

[16] R. Woodard, *Invariant formulation of and radiative corrections in quantum gravity*. PhD thesis, Harvard University, Cambridge, MA., 1984.

[17] L. C. Maximon, "The dilogarithm function for complex argument," *Proceedings of the Royal Society A: Mathematical, Physical and Engineering Sciences*, vol. 459, pp. 2807–2819, Nov. 2003.

[18] J. Hadamard, *Le problème de Cauchy et les équations aux dérivées partielles linéaires hyperboliques*. Hermann & Cie., Paris, 1932.

[19] U. Leonhardt, *Measuring the quantum state of light*. Cambridge University Press, Cambridge, England, 1997.

[20] S. Hossenfelder and L. Smolin, "Phenomenological quantum gravity," *Physics in Canada*, vol. 66, no. 2, pp. 99–102, 2010.

[21] J. Lee and R. M. Wald, "Local symmetries and constraints," *Journal Mathematical Physics*, vol. 31, no. 3, pp. 725–743, 1990.

[22] S. Deser, "Self-interaction and gauge invariance," *General Relativity and Gravitation*, vol. 1, no. 1, pp. 9–18, 1970.